Journal of Medicinal Chemistry

pubs.acs.org/jmc

Article

Discovery of Novel Pyrrolo[2,3-*d*]pyrimidine-based Derivatives as Potent JAK/HDAC Dual Inhibitors for the Treatment of Refractory Solid Tumors

Xuewu Liang, Shuai Tang, Xuyi Liu, Yingluo Liu, Qifu Xu, Xiaomin Wang, Abdusaid Saidahmatov, Chunpu Li, Jiang Wang, Yu Zhou, Yingjie Zhang, Meiyu Geng, Min Huang,* and Hong Liu*

Cite This: https://dx.doi.org/10.1021/acs.jmedchem.0c02111

Read Online

ACCESS | Metrics & More | Article Recommendations | Supporting Information

ABSTRACT: It remains a big challenge to develop HDAC inhibitors effective for solid tumors. Previous studies have suggested that the feedback activation of JAK-STAT3 pathway represents a key mechanism leading to resistance to HDAC inhibitors in breast cancer, suggesting the therapeutic promise of JAK/HDAC dual inhibitors. In this work, we discovered a series of pyrrolo[2,3-*d*]pyrimidine-based derivatives as potent JAK and HDAC dual inhibitors. Especially, compounds **15d** and **15h** potently inhibited JAK1/2/3 and HDAC1/6 and displayed antiproliferative and proapoptotic activities in triple-negative breast cancer cell lines. Besides, compounds **15d** and **15h** also diminished the activation of LIFR-JAK-STAT signaling triggered by tumor-associated fibroblasts, which suggests that these compounds could potentially overcome the drug resistance caused by the tumor microenvironment. More importantly, compound **15d** effectively inhibited the tumor growth in MDA-MB-231 xenograft tumor model. Overall, this work provides valuable leads and novel antitumor mechanisms for the treatment of the SAHA-resistant triple-negative breast cancers.

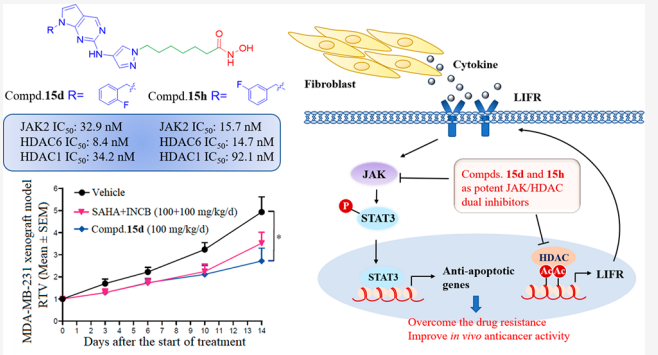

INTRODUCTION

Simultaneous intervention of two or even multiple targets in the complex pathogenesis may be beneficial to the treatment of patients suffered from complex diseases like malignant tumors and central nervous system diseases.[1,2] To tackle complex diseases like cancer, modulating the activity of multiple targets could possibly achieve better therapeutic benefit, which provides a reasonable scientific basis for multitargeted drug design.[3] In clinical applications, multitargeted drugs possess advantages such as optimal therapeutic efficacy (like sorafenib and dasatinib), slowing down drug resistance, as well as predictable pharmacokinetic (PK) profile and avoiding drug−drug interactions compared with combinational therapies.[4−6] However, it is undeniable that multitargeted effects are also a very important cause of drug side effects. Nevertheless, multitarget drug design strategies are widely used in antitumor drugs.

Histone deacetylases (HDACs), a family of epigenetic enzymes, regulate the deacetylation of a variety of their substrates including histone and nonhistone proteins, then further control the expression level of many oncogenes and apoptotic genes and hence impact many cancer cellular processes such as cell proliferation, cell migration, cell apoptosis, and angiogenesis.[7,8] Up to now, five HDAC inhibitors, namely vorinostat (SAHA), romidepsin, belinostat, panobinostat, and chidamide (approved in China) have been approved for the treatment of hematological malignancies, including refractory cutaneous T cell lymphoma (CTCL), peripheral T cell lymphoma, and multiple myeloma.[9,10] Despite the great success achieved in treatment of hematological malignancies, most of the known HDAC inhibitors used as a single agent failed to show clinical benefits in nearly all types of solid tumors,[11] including breast cancer, renal cancer,[12] prostate cancer,[13] and head and neck cancer.[14] Simultaneously inhibiting HDAC and other targets involved in the pathogenesis of solid tumors may solve the dilemma.

Actually, chimeric HDAC inhibitors, which simultaneously modulate HDAC and other targets in feedback or compensatory pathways, could provide a potential treatment for relapsing and drug-resistant cancers. Thus far, a dozen different types of chimeric HDAC inhibitors have been developed,[15] including chimeric EGFR/HDAC inhibitors,[16]

Special Issue: New Horizons in Drug Discovery - Understanding and Advancing Kinase Inhibitors

Received: December 7, 2020

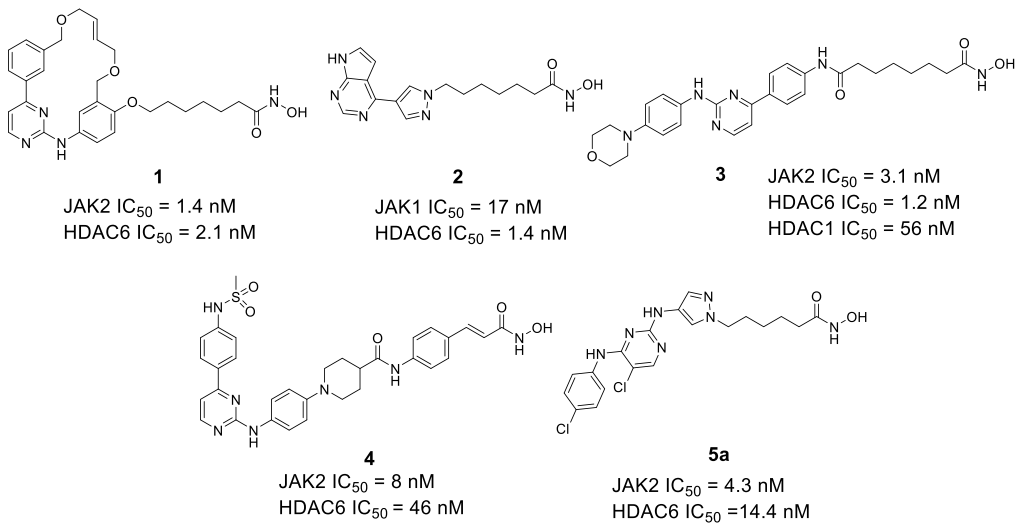

Figure 1. Chemical structures of representative JAK/HDAC dual inhibitors.

chimeric VEGFR/HDAC inhibitors,[17,18] dual c-Src/HDAC inhibitors,[19] dual Janus kinase (JAK)/HDAC inhibitors,[10] and so on.

Invasive solid tumors, such as triple-negative breast cancer, possess strong aggression, high mortality, and poor prognosis, which lack effective clinical treatment.[20,21] Development of more effective therapy for treatment of such human malignancies is very urgent. Interestingly, recent research showed that HDAC inhibitors promoted BRD4-mediated activation of leukemia inhibitory factor receptor (LIFR), which in turn activated JAK1-STAT3 signaling and restrained the efficacy of HDAC inhibitors in breast cancer.[22] Concurrent inhibition of JAK sensitized breast cancer, including the triple-negative subset, to HDAC inhibitors.[22] Thus, the development of JAK/HDAC dual inhibitors may be a reasonable and effective treatment for triple-negative breast cancer. Of note, JAKs are a family of intracellular tyrosine kinases comprising JAK1, JAK2, JAK3, and tyrosine kinase 2 (TYK2) that play a critical role in both tumor cells and in the tumor microenvironment.[23] JAKs, activated by different cytokines, lead to phosphorylation and dimerization of the signal transducers and activators of transcription (STAT) family of proteins that translocate to the nucleus and stimulate gene expression.[24−26] Inhibition of JAKs is promising to block the biological crosstalk between tumor cells and the surrounding cells in the tumor microenvironment. As such, combining JAK and HDAC is expected to overcome the limitations of HDAC inhibitors and bring clinical benefits to solid tumors. We have previously discovered that LIFR-JAK1-STAT3 signaling limits response to HDAC inhibition in the solid tumors.[22] Given JAK1 and JAK2 share the same downstream molecules in cancer cells, dual inhibition of JAK1 and JAK2 may avoid compensatory activation and ensure the blockage of the feedback activation of STAT3 signaling. Co-inhibition of HDACs with JAK1/JAK2 may be more suitable for treating solid tumors.

So far, a few JAK/HDAC dual inhibitors have been developed (Figure 1). Dymock's group first reported JAK/HDAC dual inhibitors **1**, **2**, and **3** based on the structure of JAK inhibitor templates pacritinib, ruxolitinib, and XL019, respectively.[27−29] Compound **1** was selective for JAK2 and HDAC6 against other JAK and HDAC isoforms with IC_{50} values at 1.4 and 2.1 nM. Further detailed studies in acute myelocytic leukemia (AML), multiple myeloma (MM), and erythroleukemia cell lines (EL) showed that compound **1** could effectively block both the JAK-STAT and HDAC pathways.[27] Compound **2** broadly inhibited JAK1 and HDACs 1, 2, 3, 6, and 10, with IC_{50} values of less than 20 nM. Broad cellular antiproliferative potency of compound **2** was supported by demonstration of JAK-STAT and HDAC pathway blockade in hematological cell lines.[28] It is worth mentioning that compound **3** with strong JAK2 potency (IC_{50} = 3.1 nM) and HDAC6 potency (IC_{50} = 1.2 nM) showed 16−25-fold selectivity against the other three JAK isoforms. It also showed submicromolar potencies against a panel of four solid tumor cell lines.[29] In 2018, Sheng's group reported a novel JAK/HDAC dual inhibitor **4**. Compound **4** possessed potent inhibitory activities against JAK2 and HDAC6 with IC_{50} values at 8 and 46 nM, respectively. Further studies in vivo showed that compound **4** possessed excellent antitumor efficacy in several AML models and synergized with fluconazole for the treatment of resistant *Candida albicans* infections.[30] In 2019, our group reported a novel series of pyrimidin-2-amino-pyrazol hydroxamate derivatives as JAK and HDAC dual inhibitors, among which compound **5a** possessed potent and balanced activities against both JAK2 and HDAC6 with IC_{50} values at 4.3 and 14.4 nM, respectively. Compound **5a** exhibited improved antiproliferative and proapoptotic activities over SAHA and ruxolitinib in several hematological cell lines.[31] It is worth mentioning that the studies of these JAK/HDAC dual inhibitors are more likely to focus on hematological malignancies rather than solid tumors which are insensitive to JAK inhibitors or HDAC inhibitors.

It remains a big challenge to develop HDAC inhibitors effective for solid tumors. Combining JAK and HDAC is expected to overcome the limitations of HDAC inhibitors and bring clinical benefits to solid tumors. Therefore, we developed a novel series of pyrrolo[2,3-*d*]pyrimidine-based derivatives as potent JAK/HDAC dual inhibitors and explore the advantages of multitarget drugs for the treatment of relapsing and drug-resistant cancers, in particular the triple-negative breast cancers in this work.

https://dx.doi.org/10.1021/acs.jmedchem.0c02111
J. Med. Chem. XXXX, XXX, XXX−XXX

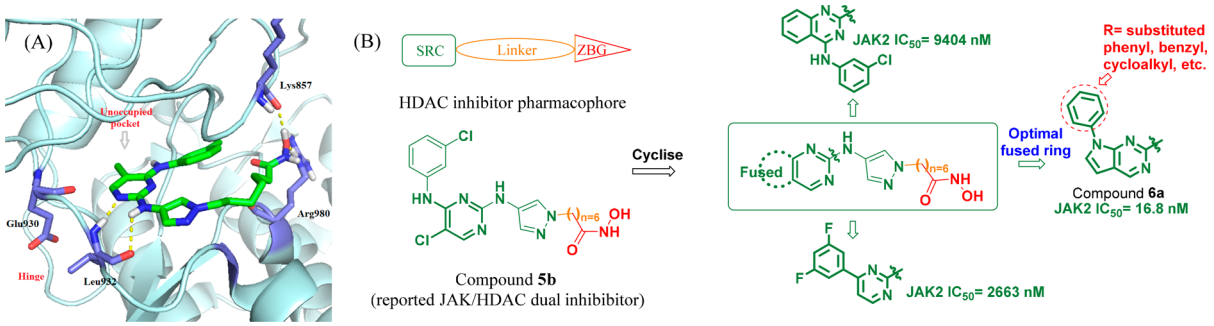

Figure 2. Rational design of novel JAK and HDAC dual inhibitors. (A) Predicted binding mode of compound **5b** in the ATP pocket of JAK2 (PDB 3FUP). The unoccupied pocket is indicated by arrow. (B) Design strategy of JAK and HDAC dual inhibitors based on compound **5b**. The three parts of HDAC inhibitor pharmacophore are indicated in three colors (ZBG, zinc-binding group). In addition, the structure of compound **6a** is shown.

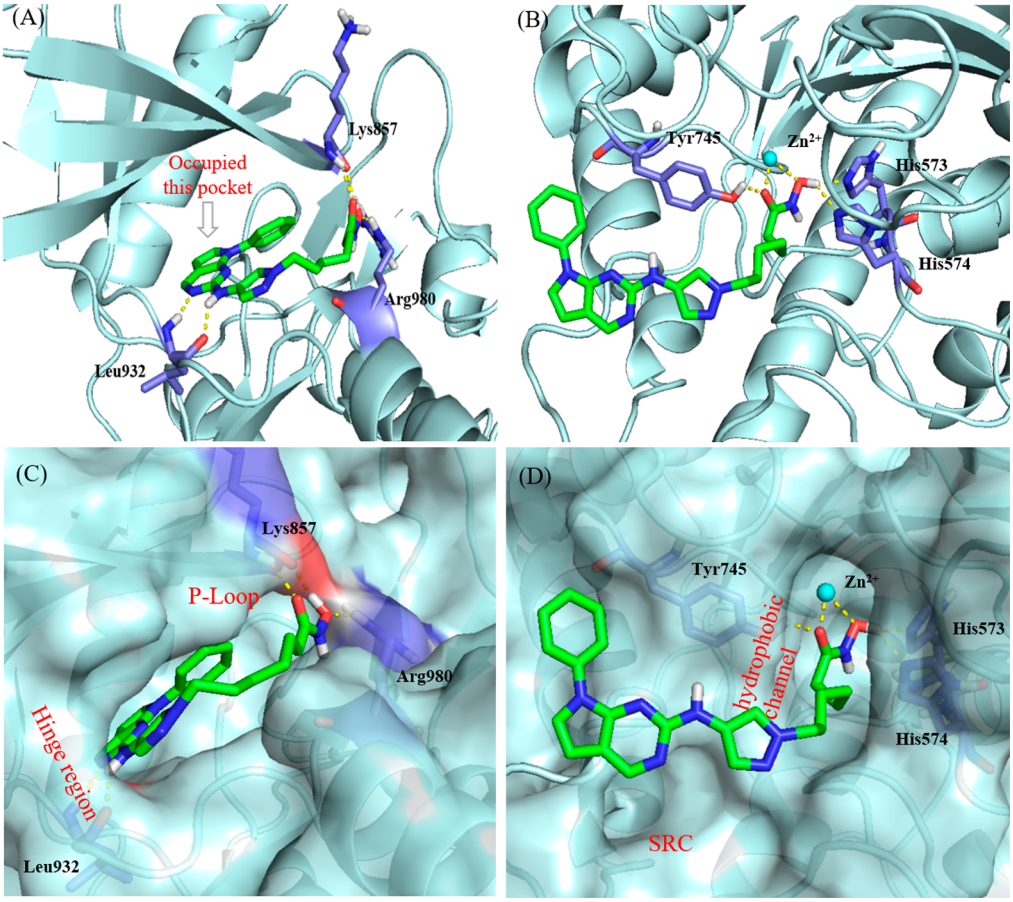

Figure 3. (A) The predicted binding mode of compound **6a** in the ATP pocket of JAK2 (PDB 3FUP). (B) The predicted binding mode of compound **6a** in the active site of HDAC6 (PDB 5EEI). (C) Surface representation of compound **6a** in the ATP pocket of JAK2 (PDB 3FUP). (D) Surface representation of compound **6a** in the active site of HDAC6 (PDB 5EEI). Yellow dashed lines represent the hydrogen bonds. In the ligand, oxygen, nitrogen, carbon, and polar hydrogen atoms are shown in red, blue, green, and white, respectively. The figures were generated using PyMol (http://www.pymol.org/).

RESULTS AND DISCUSSION

Rational Design of Novel JAK and HDAC Dual Inhibitors. In our previous research, a potent JAK/HDAC dual inhibitor **5b** with notable antiproliferative and proapoptotic activities was identified.[31] However, this series of compounds showed a very potent in vitro but a mild in vivo anticancer activities against hematological malignancies. In this work, we carried out further structural modifications based on compound **5b** in the hope of obtaining desired in vivo efficacy on the solid tumors, which are not sensitive to JAK inhibitors or HDAC inhibitors. Through analyzing the binding mode between compound **5b** and JAK2 protein using molecular docking study, we found a hydrophobic pocket in the ATP pocket of JAK2 protein that had not yet been occupied (Figure 2A). Thus, we tried to fill this hydrophobic pocket with an aromatic ring on the ligand molecule to improve the binding of ligand to protein. In addition, considering the large cavity in the surface recognition cap (SRC) of HDAC protein, the introduction of an aromatic ring on the ligand molecule would

https://dx.doi.org/10.1021/acs.jmedchem.0c02111
J. Med. Chem. XXXX, XXX, XXX−XXX

Scheme 1. Synthesis of Intermediate Compounds 11a,b[a]

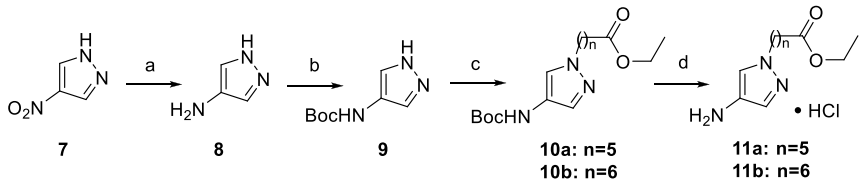

[a]Conditions and reagents: (a) Pd/C, H_2, EtOH, rt, 2 days, 90%; (b) $(Boc)_2O$, $NaHCO_3/H_2O$, THF, rt, 2 days, 75%; (c) Cs_2CO_3, CH_3CN, 40−50 °C, 10 h, 76−78%; (d) HCl/EtOAc, rt, 10 h, 63−75%.

Scheme 2. Synthesis of Intermediate Compounds 13a−s[a]

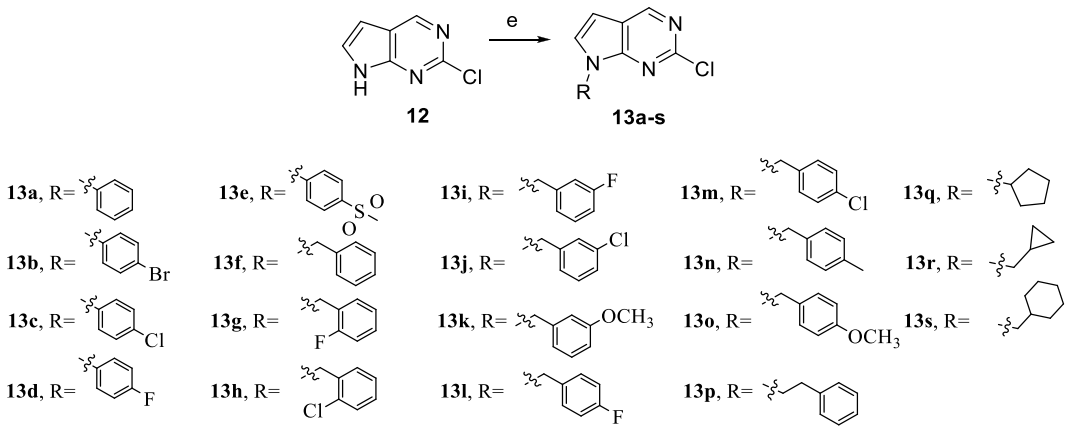

[a]Conditions and reagents: (e) for **13a−e**. CuI, *trans*-1,2-cyclohexanediamine, K_3PO_4, dioxane, 130 °C, microwave 1 h, 20−50%; For **13f−s**, K_2CO_3, CH_3CN, 40−50 °C, 5 h, 67−96%.

not affect the binding of the ligand to HDAC protein. To improve the biological activity, fused ring strategy in the ligand molecule was frequently applied in the design of JAK inhibitors.[32,33] On the basis of the above analysis, we introduced different aromatic rings to the pyrimidine ring on the compound **5b**, including phenyl ring, biphenyl ring, and pyrrole ring (Figure 2B). By preliminary inhibitory activity against JAK2, compounds containing quinazoline and phenylpyrimidine scaffolds showed weaker JAK2 inhibition than the compound containing pyrrolo[2,3-*d*]pyrimidine scaffold. Therefore, we selected pyrrole ring as the optimal fused ring to design the novel pyrrolo[2,3-*d*]pyrimidine-based derivatives as novel and potent JAK/HDAC dual inhibitors.

Compound **6a**, one of the representative pyrrolo[2,3-*d*]pyrimidine derivatives which showed the most similar structure with compound **5b**, was analyzed for its proposed binding modes in the active sites of JAK2 and HDAC6 using molecular docking study. The docking results in Figures 3(A,C) showed the binding mode of compound **6a** in the ATP active pocket of JAK2. It can be seen that aminopyrimidine moiety of compound **6a** forms dual hydrogen bonds with Leu932, which is the same as compound **5b**. As we predicted, the pyrrole ring introduced to the pyrimidine moiety perfectly fills this unoccupied hydrophobic pocket and fixes the orientation of the phenyl group. In addition, alkyl hydroxamate part of compound **6a** is projected toward the solvent region and forms hydrogen bonds with the amino acid residues Arg980 and Lys857 at the entrance of the ATP active pocket in JAK2. The docking results in Figure 3B,D showed the binding mode of compound **6a** in the active site of HDAC6. It can be seen that the hydroxamic acid group of compound **6a** chelates the Zn^{2+} in a bidentate manner and forms multiple hydrogen bonds with Tyr745, His573, and His574 residues in the deep active pocket of HDAC6 protein, which contribute to its high inhibition potency against HDAC6. The aliphatic chain occupies the hydrophobic channel, which perfectly connect hydroxamic acid group with terminal cap group. The above docking results strongly support the rationality of the design strategy of the novel pyrrolo[2,3-*d*]pyrimidine-based derivatives as potent JAK/HDAC dual inhibitors.

On the basis of the structure of compound **6a**, we further introduced some substituents on the phenyl group to investigate the influence of substituents on the biological activities and designed compounds **6b−e**. Meanwhile, we reduced the length of aliphatic linker from 6 to 5 and designed compounds **6f,g**. Considering the relatively strong rigidity of the compounds **6a−g**, we replaced the phenyl groups with different substituted benzyl groups, phenethyl groups, and cycloalkyl groups to increase their structural flexibility and designed the other target compounds (**15a−l**, **16a−j**, and **17a−c**).

Chemistry. Chemical synthesis of JAK/HDAC dual inhibitors are depicted in Schemes 1−3. 4-Nitro-1*H*-pyrazole **7**, as the starting material is reduced by hydrogen to produce 1*H*-pyrazol-4-amine **8**. Intemediate **8** is protected by Boc group to obtain intemediate **9**, which reacted with commercially available bromoalkanes under basic condition of cesium carbonate to produce intermediates **10a,b**. Boc deprotection of intermediates **10a,b** under strong acid condition gave intermediates **11a,b**, respectively (Scheme 1).[31] Intermediates **13a−s** were obtained by the reaction of 2-chloro-7*H*-pyrrolo[2,3-*d*]pyrimidine **12** as the starting material

https://dx.doi.org/10.1021/acs.jmedchem.0c02111
J. Med. Chem. XXXX, XXX, XXX−XXX

Scheme 3. Synthesis of Target Compounds 6a−g, 15a−l, 16a−j, and 17a−c[a]

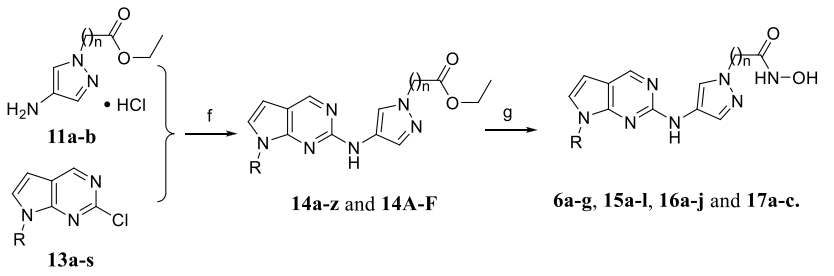

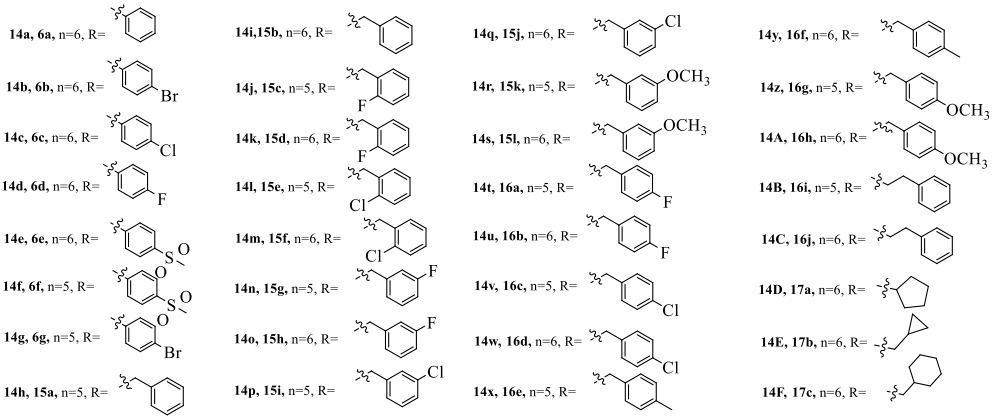

[a]Conditions and reagents: (f) EtOH, 130 °C, microwave 2 h, 18−41%; (g) NH_2OK, CH_3OH, rt, 0.5−1 h, 70−95%.

with different aryl bromides under different conditions (Scheme 2). Intermediates **14a−z** and **14A−F** were prepared by the reaction of the key intermediates **13a−s** and the key intermediates **11a,b** under the conditions of high temperature and acid catalyst in microwave apparatus. Intermediates **14a−z** and **14A−F** were subsequently reacted with NH_2OK/methanol solution to give target compounds **6a−g**, **15a−l**, **16a−j**, and **17a−c**, respectively (Scheme 3).

In Vitro JAK and HDAC Inhibition Assay. The inhibitory activities of these novel pyrrolo[2,3-*d*]pyrimidine-based derivatives against JAK2 and HDAC6 were evaluated by determining their IC_{50} values, with the approved JAK inhibitor ruxolitinib (INCB) and approved hydroxamic acid-based HDAC inhibitor SAHA as positive controls. The results in Table 1 showed that **6a** exhibited potent JAK2 and HDAC6 inhibitory activities with IC_{50} values at 16.8 and 13.1 nM, validating the rationality of our JAK and HDAC dual inhibitor design strategy shown in Figure 2. It is worth noting that compound **6a** showed much more potent HDAC6 inhibitory activity than that of SAHA (IC_{50} value: 75.9 nM) and slightly weaker JAK2 inhibitory activity than that of ruxolitnib (IC_{50} value: 2.9 nM). Simultaneously inhibiting JAK2 and HDAC6 with nanomolar level is acceptable. Next, different *para*-substituents were introduced to the phenyl moiety of compound **6a**, leading to the compounds **6b−e**. Comparing JAK2 and HDAC6 inhibitory activities data of compounds **6b−e** with that of compound **6a**, it is obvious to figure out that the introduction of different *para*-substituents to the phenyl moiety will slightly reduce the JAK2 and HDAC6 inhibitory activities, excluding compound **6e**. Compound **6e** exhibited comparable JAK2 inhibitory activity to **6a** (IC_{50} values: 15.7 vs 16.8 nM) and a little more potent HDAC6 inhibitory activity than **6a** (IC_{50} values: 5.9 vs 13.1 nM). To investigate the effects of the linker on JAK2 and HDAC6 inhibition, we reduced the length of aliphatic linker from 6 to 5 and obtained compounds **6f,g**. Comparing their JAK2 and HDAC6 inhibitory activities data, we found that aliphatic linker length of 5 or 6 methylenes had no dramatic influence on the JAK2 and HDAC6 inhibition. All the compounds (**6a−g**) containing 5 or 6 methylenes showed high potencies on the JAK2 and HDAC6 inhibition. Linker length of 5 or 6 methylenes is both accepted in the structural modification of these JAK/HDAC dual inhibitors.

To reduce the rigidity of compounds **6a−g** and considering the aliphatic linker length of 5 or 6 methylenes both accepted, compounds **15a−l** and compounds **16a−j** were synthesized and evaluated. Compounds **15a−j** exhibited potent JAK2 and HDAC6 inhibition with IC_{50} values lower than 50 nM (Table 1), validating that *ortho*- and *meta*- halogen substituents on the phenyl moiety were well tolerated both in the JAK2 and HDAC6 inhibition. However, compounds **15k−l** exhibited poor JAK2 inhibition (IC_{50} > 100 nM) and potent HDAC6 inhibition (IC_{50} lower than 50 nM), validating that *meta*-methoxyl substituent on the phenyl moiety was not tolerated in the JAK2 inhibition. Note that through this round of compound screening, we obtained many potent JAK/HDAC dual inhibitors with IC_{50} at nanomolar level, including **15a**, **15c−e**, and **15g−i**. Among these compounds, **15g** potently inhibited JAK2 and HDAC6 with the IC_{50} values at 4.1 and 13.7 nM, respectively.

Next, *para*-substituents were introduced to the phenyl moiety on the structures of JAK/HDAC dual inhibitors **15a** and **15b**. The enzyme inhibition results in Table 2 showed that *para*-substituents (no matter halogen or methoxyl group) on the phenyl moiety were not beneficial for JAK2 inhibition but tolerated in HDAC6 inhibition. All compounds **16a−h** exhibited very poor JAK2 inhibition (IC_{50} > 100 nM), which is not what we expected. In addition, both compounds **16i,j**

https://dx.doi.org/10.1021/acs.jmedchem.0c02111
J. Med. Chem. XXXX, XXX, XXX−XXX

Table 1. Structures and in Vitro Enzymes Inhibitory Activities Comparison of the Target Compounds 6a−g and Compounds 15a−l[a]

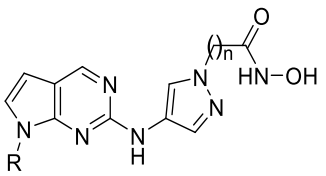

Compd.	Structure		JAK2	HDAC6
	R	n	IC_{50} (nM)	IC_{50} (nM)
6a		6	16.8±2.0	13.1±2.5
6b		6	54.8±2.6	20.2±0.8
6c		6	48.2±0.1	33.4±0.1
6d		6	32.9±1.3	21.6±4.3
6e		6	15.7±0.8	5.9±0.3
6f		5	9.8±0.2	10.8±1.3
6g		5	17.5±3.3	11.3±0.6
15a		5	33.0±1.3	13.8±0.7
15b		6	51.0±1.2	12.5±3.8
15c		5	10.0±0.3	15.3±0.7
15d		6	32.9±8.2	8.4±0.5
15e		5	24.8±2.3	45.0±7.0
15f		6	30.8±0.1	41.5±8.4
15g		5	4.1±0.7	13.7±1.0
15h		6	15.7±3.7	14.7±2.4
15i		5	17.7±6.7	34.4±7.6
15j		6	39.8±4.8	36.8±8.5
15k		5	123.9±22.1	37.6±3.3
15l		6	209.2±18.1	28.8±2.2
SAHA	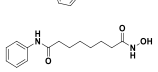		NA[b]	75.9±5.2
Ruxolitinib (INCB)	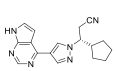		2.9±0.3	NA[b]

[a]Assays were performed in replicate ($n \geq 3$), IC_{50} values are shown as mean ± SD. [b]Not active at 10 μM.

Table 2. Structures and in Vitro Enzymes Inhibitory Activities Comparison of the Target Compounds 16a−j and Compounds 17a−c[a]

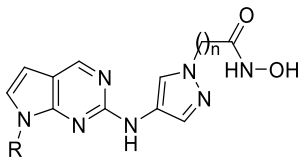

Compd.	Structure		JAK2	HDAC6
	R	n	IC_{50} (nM)	inhibition rate @ 10 nM[b]
16a		5	>100	46%
16b		6	>100	62%
16c		5	>100	38%
16d		6	>100	39%
16e		5	>100	34%
16f		6	>100	38%
16g		5	>100	46%
16h		6	>100	40%
16i		5	>100	41%
16j		6	>100	49%
17a		6	>100	22[c]
17b		6	>100	16[c]
17c		6	69	88[c]
SAHA	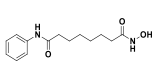		NA[d]	75.9[c]
Ruxolitinib (INCB)	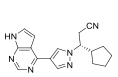		2.9	NA[d]

[a]Assays were performed in replicate ($n \geq 3$). [b]@10 nM means HDAC6 inhibition rate at 10 nM. [c]The IC_{50} (nM) values of compounds **17a**, **17b**, **17c**, and SAHA against HDAC6. [d]Not active at 10 μM.

exhibited very poor JAK2 inhibition (IC_{50} > 100 nM), validating that phenethyl group in R substituent were also not beneficial for JAK2 inhibition but tolerated in HDAC6 inhibition.

Finally, we also introduced some cycloalkyl substituents instead of aromatic substituents as R group to the pyrrolo moiety of the JAK/HDAC dual inhibitors, leading to the compounds **17a−c**. The enzyme inhibition results in Table 2 showed that compounds **17a** and **17b** possessed very potent inhibitory activities against HDAC6 (IC_{50}: 22 and 16 nM,

https://dx.doi.org/10.1021/acs.jmedchem.0c02111
J. Med. Chem. XXXX, XXX, XXX−XXX

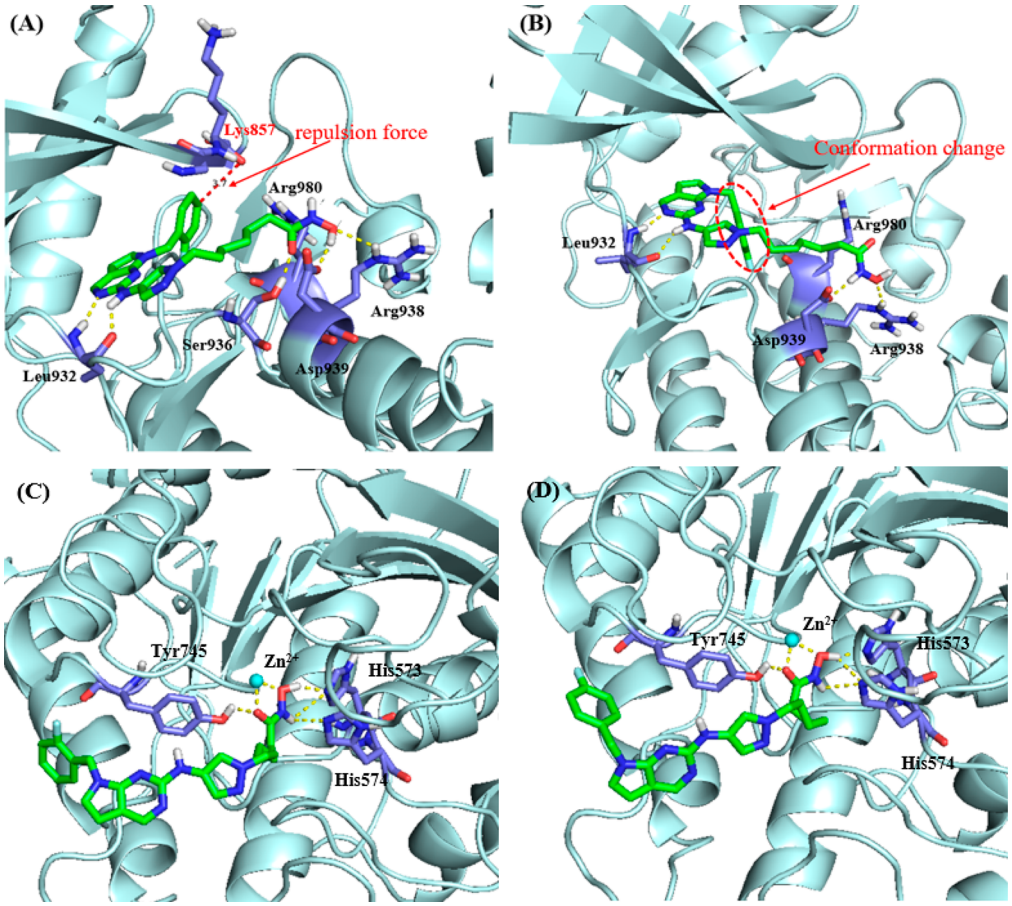

Figure 4. (A) Predicted binding mode of compound **15d** in the ATP pocket of JAK2 (PDB 3FUP). (B) Predicted binding mode of compound **16b** in the ATP pocket of JAK2 (PDB 3FUP). (C) Predicted binding mode of compound **15d** in the active site of HDAC6 (PDB 5EEI). (D) Predicted binding mode of compound **16b** in the active site of HDAC6 (PDB 5EEI). Yellow dashed lines represent the hydrogen bonds. In the ligand, oxygen, nitrogen, carbon, fluoro, and in polar hydrogen atoms are shown in red, blue, green, pale cyan, and white, respectively. The repulsion force between the ligand molecule with the Lys857 residue of JAK2 protein was shown in a red dashed line. The figures were generated using PyMol (http://www.pymol.org/).

Table 3. JAK Isoform and HDAC Selectivity Profiles of Representative Compounds[a]

	JAK2	JAK1	JAK3	TYK2	HDAC1	HDAC6
compd	IC_{50} (nM)	IC_{50} (nM)	IC_{50} (nM)	IC_{50} (nM)	IC_{50} (nM)	IC_{50} (nM)
6a	16.8 ± 2.0	19.6 ± 3.2	81.2 ± 4.8	23.5 ± 0.2	52.1 ± 0.9	13.1 ± 2.5
15c	10.0 ± 0.3	32.3 ± 8.6	18.4 ± 3.1	13.3 ± 4.3	144.7 ± 23.7	15.3 ± 0.7
15d	32.9 ± 8.2	33.4 ± 4.0	25.1 ± 0.2	40.9 ± 3.3	34.2 ± 1.3	8.4 ± 0.5
15g	4.1 ± 0.7	8.7 ± 1.0	12.6 ± 1.9	15.0 ± 3.3	172.9 ± 11.0	13.7 ± 1.0
15h	15.7 ± 3.7	19.9 ± 2.4	16.1 ± 0.1	21.7 ± 1.8	92.1 ± 19.1	14.7 ± 2.4
Ruxolitinib	2.9 ± 0.3	1.1 ± 0.1	20.7 ± 0.9	10.3 ± 5.1	ND[b]	ND
SAHA	ND	ND	ND	ND	180.3 ± 10.9	75.9 ± 5.2

[a]Assays were performed in replicate ($n \geq 3$), IC_{50} values are shown as mean ± SD. [b]Not determined.

respectively) but very low inhibitory activities against JAK2 (IC_{50} > 100 nM). However, compound **17c** possessed a balanced but mild JAK2 and HDAC6 inhibition with the IC_{50} values at 69 and 88 nM, respectively.

The inhibitory activities of the corresponding compounds **16a−h** against JAK2 were greatly decreased when the *para*-substituents were present on the phenyl moiety. To explain the phenomenon, we analyzed the binding modes of compound **15d** and compound **16b** in the ATP pocket of JAK2 (Figure 4). The docking results in Figure 4A showed that, like compound **6a**, compound **15d** showed a similar binding mode with JAK2 protein. Aminopyrimidine moiety of compound **15d** forms dual hydrogen bonds with Leu932 and alkyl hydroxamate moiety forms multiple hydrogen bonds with the amino acid residues Ser936, Arg938, and Asp939. Therefore, compound **15d** exhibited comparable and potent JAK2 inhibitory activity to **6a** (IC_{50} values: 32.9 vs 16.8 nM). It is worth noting that the *para*-site of the phenyl moiety in the ligand molecule **15d** was very close (3.7 Å, indicated by a red dashed line) to the Lys857 residue at the P-loop region. The introduction of a substituent in the *para*- site of the phenyl moiety may aggravate the repulsion force between the ligand molecule with the Lys857 residue of JAK2 protein. Therefore, in the binding mode of compound **16b** with JAK2 protein

https://dx.doi.org/10.1021/acs.jmedchem.0c02111
J. Med. Chem. XXXX, XXX, XXX−XXX

Table 4. Further HDAC Selectivity Data for Representative Lead 15d[a]

	HDAC class I			HDAC class IIa		HDAC class IIb	
	HDAC1	HDAC3	HDAC8	HDAC4	HDAC7	HDAC6	HDAC10
compd	IC_{50} (nM)	IC_{50} (nM)	IC_{50} (nM)	IC_{50} (nM)	IC_{50} (nM)	IC_{50} (nM)	IC_{50} (nM)
15d	34.2 ± 1.3	3.8 ± 0.5	9.2 ± 0.8	>10000	>10000	8.4 ± 0.5	3.6 ± 0.4
SAHA	180.3 ± 10.9	28.1 ± 1.6	191.5 ± 24.7	63.2 ± 7.7	75.2 ± 10.9	75.9 ± 5.2	47.5 ± 3.5

[a]Assays were performed in replicate ($n \geq 3$), IC_{50} values are shown as mean ± SD.

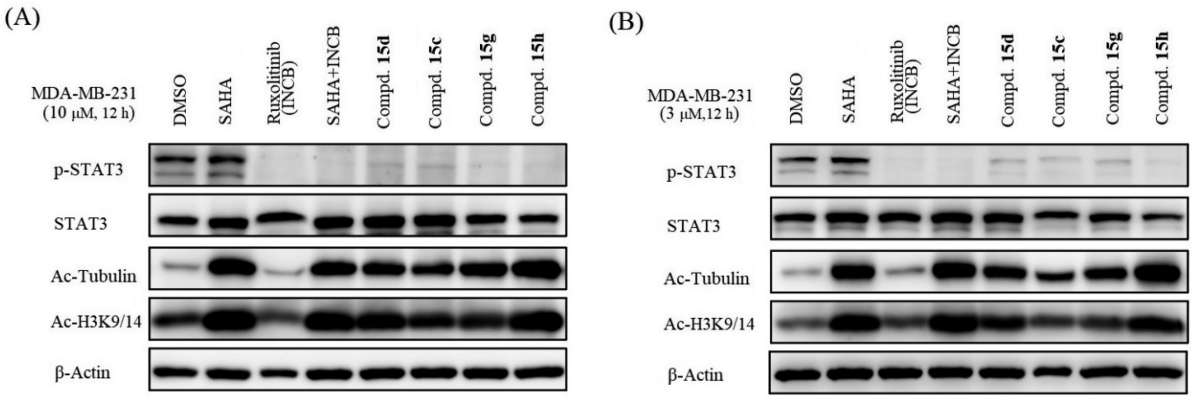

Figure 5. (A) MDA-MB-231 cells were treated with DMSO or compounds at 10 μM for 12 h. (B) MDA-MB-231 cells were treated with DMSO or compounds at 3 μM for 12 h. The levels of phosphorylated STAT3 (p-STAT3-Tyr705), STAT3, acetyl-α-tubulin (Ac-tubulin), acetyl-H3K9/14 (Ac-H3K9/14) were determined by immunoblotting. β-Actin was used as a loading control. Ruxolitinib was indicated by INCB in the combined treatment group.

(Figure 4B), the dominant conformation of the phenyl moiety in the ligand molecule **16b** has undergone a huge change. The disadvantageous conformation change led to a sharp decrease in the JAK2 inhibitory activity of the ligand molecules (IC_{50} > 100 nM). In addition, compound **15d** showed a similar binding mode with **16b** in the active site of HDAC6 (Figure 4C,D), which rationally confirmed the comparable and potent HDAC6 inhibitory activity of compounds **15d** (IC_{50} = 8.4 nM) and **16b** (62% inhibition at 10 nM).

In summary, we did a relatively comprehensive structure–activity relationship (SAR) study based on the linker length and R group. Aliphatic linker length of 5 or 6 methylenes, *para*-substituted phenyl, *ortho*-, and *meta*- halogen substituted benzyl groups were accepted in this series of potent JAK/HDAC dual inhibitors.

JAK and HDAC Selectivity Profile. Because of their significant JAK2 and HDAC6 inhibitory activities, Compounds **6a**, **15c**, **15d**, **15g**, and **15h** were evaluated against JAK isoforms and HDAC isoforms to perform the JAK and HDAC selectivity profile. As depicted in Table 3, this series of compounds exhibited potent but undifferentiated inhibitory activities against JAK1, JAK2, JAK3, and TYK2 with the IC_{50} values between 4 and 40 nM (except that compound **6a** showed a mild inhibitory activity against JAK3 with the IC_{50} value of 81.2 nM). Therefore, from the experimental results, these compounds tend to be pan-JAKs inhibitors. A comprehensive HDAC selectivity study on the representative compounds was also conducted. Results in Tables 3 and 4 showed that compounds **6a**, **15c**, **15d**, **15g**, and **15h** all exhibited potent inhibitory activities against HDAC1 and HDAC6. Especially, compound **15d** broadly inhibited HDAC class I (HDACs 1, 3, 8), and HDAC class IIb (HDACs 6, 10), with IC_{50} values of less than 50 nM. However, compound **15d** possessed very poor inhibitory activities against HDAC class IIa (HDACs 4, 7), with IC_{50} values of larger than 10 μM (Table 4).

Concurrent Inhibition of Intracellular JAK and HDAC. To confirm the intracellular dual actions of this series of JAK/HDAC dual inhibitors, Western blot analysis was performed. As the previous literature reported that concurrent inhibition of BRD4 or JAK sensitized breast cancer to HDAC inhibitors, we selected triple-negative breast cancer cell line MDA-MB-231 to perform the Western blot. Consistent with our previous findings, HDAC inhibitor SAHA at the concentration of 10 and 3 μM could cause the upregulation of phosphorylated STAT3, suggesting the restrained efficacy in breast cancer. Cotreatment of HDAC inhibitor SAHA with JAK inhibitor ruxolitinib (INCB) successfully suppressed the JAK-STAT pathway. To our delight, at the concentration of 10 μM, our designed compounds **15c**, **15d**, **15g**, and **15h** obviously increased the HDAC substrates acetyl-α-tubulin and acetyl-histone H3, suggesting the effective of HDACs activity and meanwhile prevented the feedback activation of phosphorylated STAT3 in a dose-dependent manner compared to the control group, which validated that this series of newly designed compounds simultaneously inhibited JAKs and HDACs in MDA-MB-231 cells (Figure 5A). At the low concentration of 3 μM, compounds **15c**, **15d**, **15g**, and **15h** also effectively simultaneously inhibited JAK and HDAC proteins in the MDA-MB-231 cell lines (Figure 5B). In this celluar assay, the inhibitory activities against JAK and HDAC proteins of compounds **15d** and **15h** were more potent than that of compounds **15c** and **15g**.

Considering their potent inhibitory activities against JAK and HDAC proteins in MDA-MB-231 cell lines, we further verified the effect of the compounds **15d** and **15h** on the inhibition of the two target proteins JAK and HDAC in the triple-negative breast cancer cell line BT-549. The results in

https://dx.doi.org/10.1021/acs.jmedchem.0c02111
J. Med. Chem. XXXX, XXX, XXX−XXX

Figure 6 showed that similarly to results obtained in MDA-MB-231 cells, compounds **15d** and **15h** increased the levels of

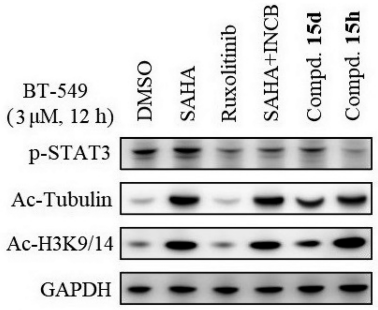

Figure 6. BT-549 cells were treated with DMSO or compounds at 3 μM for 12 h. The levels of phosphorylated STAT3 (*p*-STAT3-Tyr705), acetyl-α-tubulin (Ac-tubulin), and acetyl-H3K9/14 (Ac-H3K9/14) were determined by immunoblotting. GAPDH was used as a loading control. Ruxolitinib was indicated by INCB in the combined treatment group.

HDAC substrates, Ac-tubulin, and Ac-H3K9/14 yet did not cause the feedback activation of of p-STAT3 at the concentration of 3 μM, which further confirmed the JAK and HDAC dual inhibitory activity of the newly designed compounds at the cellular level.

In Vitro Antiproliferation Assay. JAK/HDAC dual inhibitors reported before tended to focus on hematological malignancies rather than solid tumors which were insensitive to JAK inhibitors or HDAC inhibitors. To further investigate the antiproliferative effect of these JAK/HDAC dual inhibitors on solid tumors, we selected hepatoma, renal cell adenocarcinoma, nonsmall cell lung carcinomas, colon cancer, and other three breast cancer cell lines as the research objects. The results in Supporting Information, Table S1, showed that most of our dual inhibitors, especially the compounds **6a**, **15d**, and **15h**, exhibited better antiproliferative activities against 4T1 and MDA-MB-231 breast cancer cell lines than other solid cancer cell lines. The antiproliferative results preliminarily validated that our designed compounds may provide an effective treatment for intractable breast cancers.

Encouraged by the cell-based anticancer activity in breast cancer cells, we continue to select several breast cancer cells for further antiproliferative activity test. Results in Table 5 showed

Table 5. In Vitro Antiproliferative Activities of Representative Compounds on the Breast Cancer Cells[a]

	antiproliferative effect on breast cancer cells (IC_{50}, μM)				
compd	4T1	MDA-MB −231	BT-549	MDA-MB-468	Cal-51
15d	2.87	3.83	2.41	2.08	0.79
15h	3.72	3.94	3.02	2.45	1.28
SAHA	1.59	1.09	2.96	2.75	1.04

[a]Assays were performed in replicate ($n \geq 3$).

that compounds **15d** and **15h** not only showed potent antiproliferative activities against the breast cancers 4T1 and MDA-MB-231, with the IC_{50} values at the low digit micromolar level, but also inhibited the growth of BT-549, MDA-MB-468, and Cal-51 breast cancer cells. Meanwhile, in the BT-549 (IC_{50} values: 2.41 vs 2.96 μM), MDA-MB-468 (IC_{50} values: 2.08 vs 2.75 μM), and Cal-51 breast cancer cells (IC_{50} values: 0.79 vs 1.04 μM), the antiproliferative activity of compound **15d** is slightly better than that of SAHA.

Apoptosis Assay. Because compound **15d** exhibited excellent antiproliferative activity in breast cancer cells, we continue to select this compound for further studies on its pro-apoptotic activity via flow cytometry. Results in Figure 7 showed that at the concentration of 2.5 μM, SAHA induced about 39% MDA-MB-231 cell apoptosis and possessed synergistic pro-apoptotic activity in combination with ruxolitinib (SAHA+ ruxolinib, about 72% MDA-MB-231 cell apoptosis). To our delight, compound **15d** induced MDA-MB-231 cell apoptosis in a dose-dependent manner. At the concentrations of 10 and 5 μM, compound **15d** could induce about 75% and 62% MDA-MB-231 cell apoptosis, suggesting a potent pro-apoptotic activity in MDA-MB-231 cells.

Next, we further investigate the potency of compound **15d** in inducing cell apoptosis in the 4T1 cell lines. Results in Figure 8 showed that compound **15d** induced 4T1 cell apoptosis in a dose-dependent manner. At the concentration of 5 μM, SAHA showed a very low pro-apoptotic potency on the 4T1 cell lines (about 20% 4T1 cell apoptosis). To our delight, at the same concentration of 5 μM, compound **15d** could induce about 90% 4T1 cell apoptosis, which is higher than that of SAHA and ruxolitinib combination group (about 35% 4T1 cell apoptosis). Therefore, it can be seen that for 4T1 solid tumor, compound **15d** as a JAK and HDAC dual inhibitor exhibited higher pro-apoptotic activity than the drugs combination group.

Blockage of LIFR-JAK-STAT Signaling Pathway Stimulated by the Crosstalk between Tumor Cells and Tumor Associated Fibroblasts. In addition to tumor cells, other cell components in the tumor microenvironment could also contribute to JAK-STAT signaling activation via secreting of IL-6 family of cytokines, such as LIF, leading to the activation of JAK-STAT signaling, which also contributes to the limited efficacy of HDAC inhibitors in breast cancer. Tumor associated fibroblast cells could secrete cytokines like LIF to activate JAK-STAT pathway. To investigate the effect of tumor microenvironment on HDAC inhibitor resistance in MDA-MB-231 cancer cells, we treated MDA-MB-231 cancer cells with the conditioned medium derived from tumor-associated Wl-38 fibroblasts. The results in Figure 9A,B showed that cytokines secreted by fibroblasts Wl-38 could upregulate the LIFR-JAK-STAT signaling pathway in MDA-MB-231 cancer cells. In the represence of conditioned medium, HDAC inhibitor SAHA further substantially amplified LIFR-JAK-STAT signaling pathway, presumably rendering tumors more resistant to drug. To our delight, at 3 μM, compounds **15d** and **15h** effectively diminished the LIFR-JAK-STAT signaling pathway, which demonstrated the potential therapeutic benefits of JAK and HDAC dual inhibitors in triple-negative breast cancer and provided a reasonable basis for the advantages in the in vivo experiment.

Preliminary in Vivo Antitumor Activity Evaluation. Considering its potent antiproliferative and proapoptotic capacities in MDA-MB-231 breast cancer cell lines, compound **15d** was progressed into a preliminary in vivo antitumor activity study in a MDA-MB-231 xenograft model. Mice were randomly separated into six groups (n = 6/group) and treated with compound **15d** (30 or 100 mg/kg/day, IP), SAHA (100 mg/kg/day, PO), ruxolitinib (100 mg/kg/day, PO), combination of SAHA and ruxolitinib (100 + 100 mg/kg/day, PO) and saline for 14 consecutive days. Tumor growth inhibition

https://dx.doi.org/10.1021/acs.jmedchem.0c02111
J. Med. Chem. XXXX, XXX, XXX−XXX

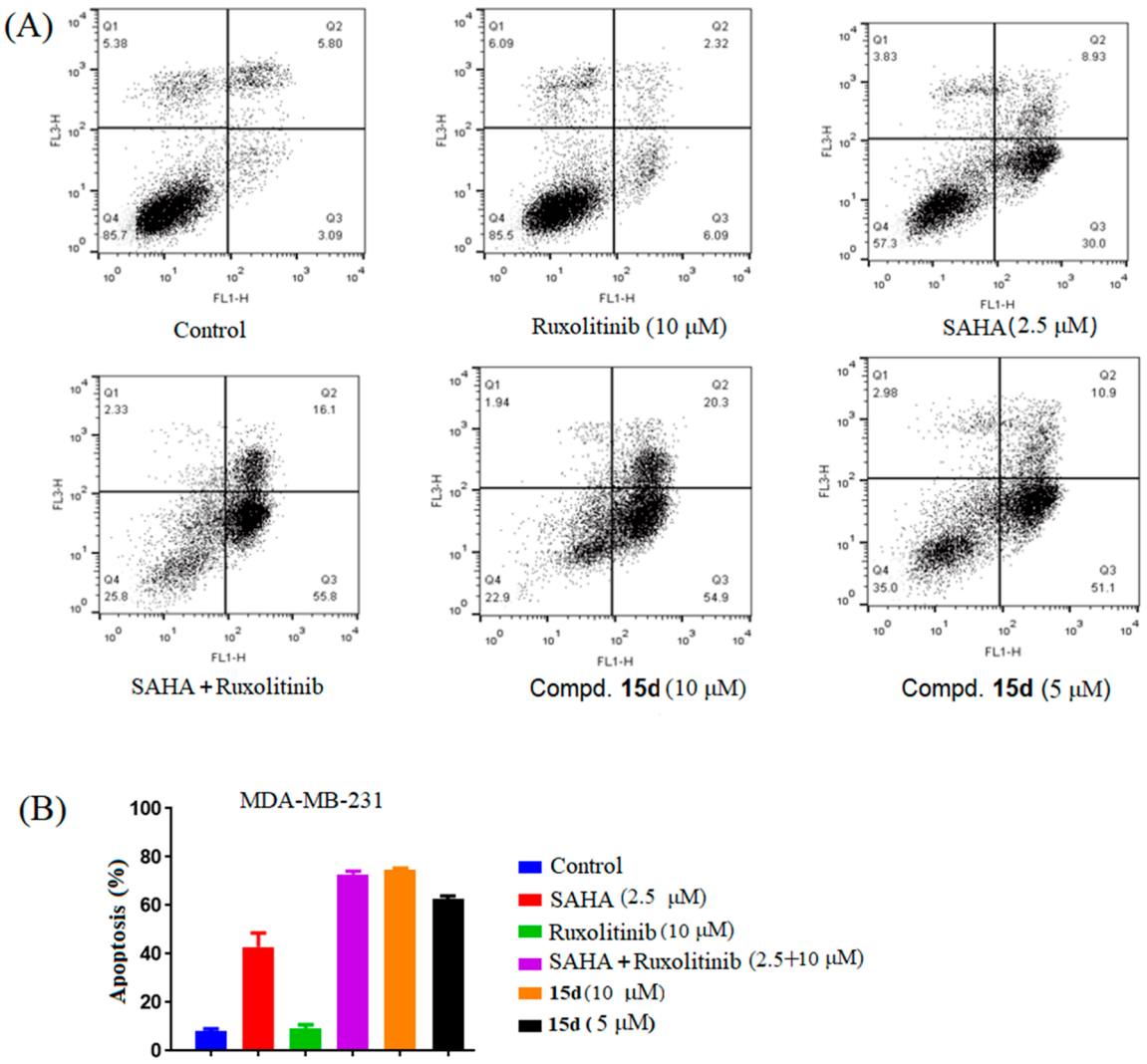

Figure 7. (A) Induction of apoptosis in MDA-MB-231 cells after 48 h of treatment. (B) Efficacy of compound **15d** at different concentrations to induce apoptosis in MDA-MB-231 cells after 48 h of treatment.

(TGI) was calculated at the end of treatment. As shown in Table 6 and Figure 10, compound **15d** showed significant antitumor potency with TGI of 37% at the low dose of 30 mg/kg/day and 49% at the large dose of 100 mg/kg/day. The antitumor activity of compound **15d** is comparable to or slightly better than that of the combination group SAHA and Ruxolitinib. In addition, the body weight of mice in the low-dose administration (30 mg/kg/d, IP) group of compound **15d** did not change significantly, but the mice in the high-dose administration group (100 mg/kg/d, IP) showed some weight loss (about 15%). Nevertheless, the result indicated that compound **15d** as a potent JAK and HDAC dual inhibitor exhibited effective antitumor activity in vivo against triple-negative breast cancer.

Protein Kinase Selectivity Profile. Because of its potent JAK/HDAC dual inhibitory activities and anticancer capacities, compound **15d** was further tested against 134 kinases to characterize its protein kinase selective profiles at 50 and 500 nM, respectively. As depicted in Supporting Information, Table S2 and Figure 11, at the concentration of 50 nM, compound **15d** exhibited over 75% inhibition of JAK1, JAK2, JAK3, and TYK2, which further confirmed that compound **15d** is a pan-JAK inhibitor. In addition, compound **15d** exhibited 65% inhibition of FMS-like receptor tyrosine kinase 3 (Flt3), which plays important roles in the progress of tumors. Although compound **15d** possessed strong inhibitory activities against other kinases, such as VEGFR-2, Met, FGFR at 500 nM, overall, compound **15d** was relatively selective to the inhibition of JAK.

CONCLUSION

It is urgent to develop a more effective therapy for the treatment of invasive solid tumors, especially triple-negative breast cancer. In the present work, a novel series of pyrrolo[2,3-*d*]pyrimidine-based derivatives simultaneously inhibiting JAKs and HDACs were rationally designed, synthesized, and evaluated. Most of these compounds possessed JAK/HDAC dual inhibitory activities with IC_{50} values at nanomolar levels. Lead **15d**, as the representative compound, showed the potent antiproliferative and proapoptotic activities in several breast cancer cell lines. Western blot analysis confirmed that the newly designed compounds effectively and simultaneously inhibited JAK and HDAC proteins in the breast cancer cell lines. Besides, compounds **15d** and **15h** effectively downregulated the LIFR-JAK-STAT signaling pathway via the inhibition of phosphorylated STAT3, which implies that JAK/

https://dx.doi.org/10.1021/acs.jmedchem.0c02111
J. Med. Chem. XXXX, XXX, XXX−XXX

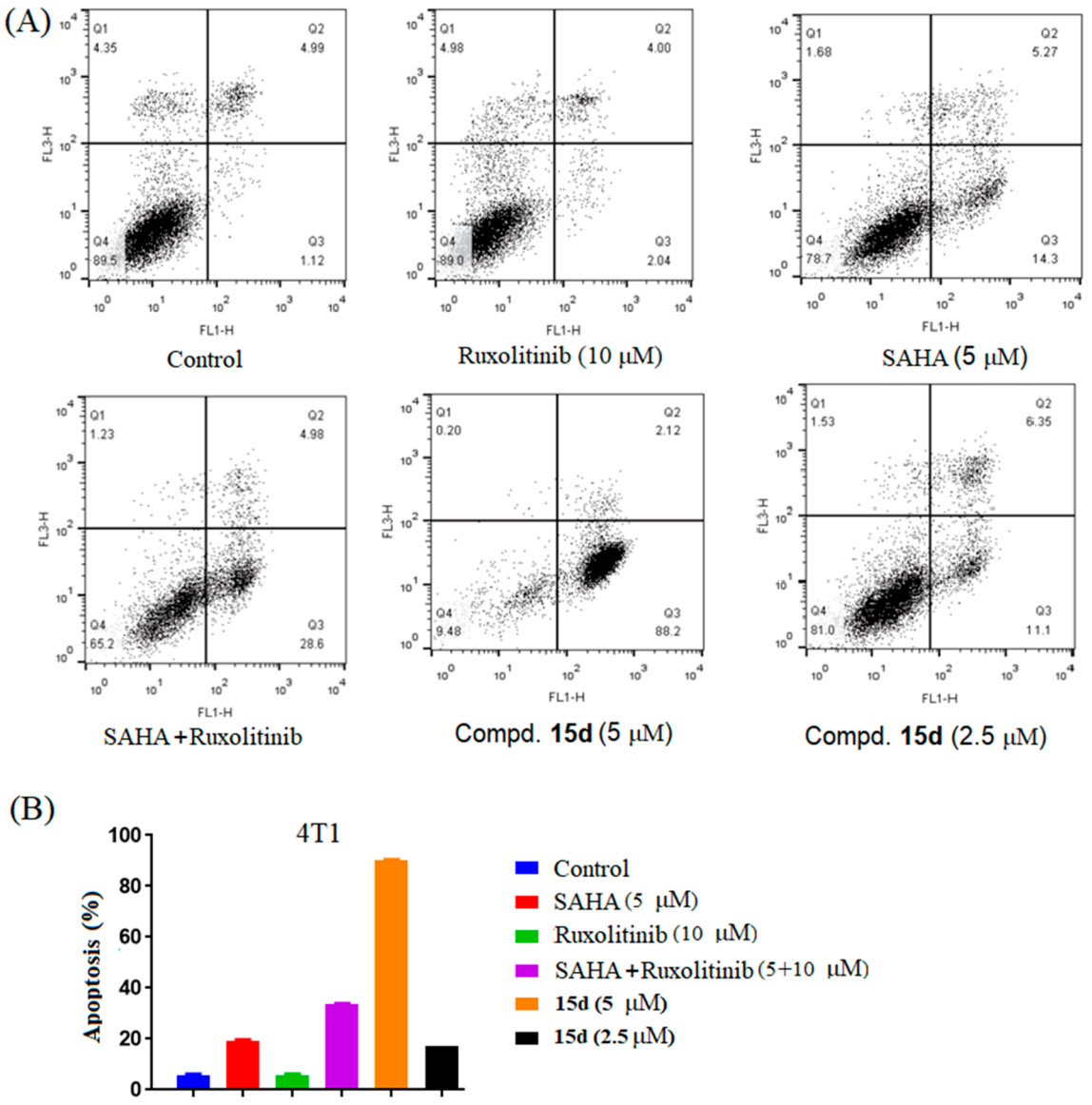

Figure 8. (A) Induction of apoptosis in 4T1 cells after 48 h of treatment. (B) Efficacy of compound **15d** at different concentrations to induce apoptosis in 4T1 cells after 48 h of treatment.

HDAC dual inhibitors can effectively overcome the drug resistance caused by the tumor microenvironment. More importantly, **15d** effectively inhibits tumor growth in MDA-MB-231-bearing mice. In summary, this work confirms the therapeutic potency of JAK and HDAC dual inhibitors and proposes a novel constructive antitumor mechanism for solid tumors.

EXPERIMENTAL SECTION

Chemistry. Unless otherwise noted, all solvents and reagents were commercially available (Sinopharm, Bide, Adamas-beta, SigmaAldrich, TCI, J&K, etc.) and used without further purification. All reactions were monitored by thin-layer chromatography on 0.25 mm silica gel plates (60 GF-254) and visualized with UV light, or iodine vapor. ^{1}H NMR and ^{13}C NMR were generated in $CDCl_3$, DMSO-d_6, or CD_3OD on Varian Mercury 300, 400, or 500 NMR spectrometers. Chemical shifts were reported in parts per million (ppm). Multiplicity of ^{1}H NMR signals was reported as single (s), double (d), triplet (t), quarter (q), and multiplet (m). ESI (Low resolution mass spectra) were recorded on a Thermo Fisher LCQ-DECA spectrometer; ESI (high resolution mass spectra) were determined on an Agilent G6520 Q-TOF spectrometer. Melting points were determined on an electrothermal melting point apparatus and were uncorrected. All the final compounds achieved a minimum of 95% purity determined by HPLC analysis, which was carried out on an Agilent 1200 coupled with a diode array detector (DAD) and an extended C18 column (4.6 mm × 250 mm, 5 μm).

*General Procedure for the Preparation of **6a**–**6g**. N-Hydroxy-7-(4-((7-phenyl-7H-pyrrolo[2,3-d]pyrimidin-2-yl)amino)-1H-pyrazol-1-yl)heptanamide (**6a**).* A mixture of ethyl 7-(4-((7-phenyl-7*H*-pyrrolo[2,3-*d*]pyrimidin-2-yl)amino)-1*H*-pyrazol-1-yl)heptanoate (**14a**, 0.20 g, 0.46 mmol) in NH_2OK/CH_3OH (20 mL) was stirred at room temperature for 0.5 h. When TLC showed the reaction was completed, evaporation of the solvent under reduced pressure gave a residue, which was dissolved in water (20 mL). the mixture was neutralized by adding a 1 M HCl solution. The white precipitate was filtered and dried in cabinet drier to give the crude material. MeOH (3–5 mL) was added and the slurry was sonicated and then stirred at 40 °C for 4 h. The solids were collected by suction filtration and allowed to air-dry overnight to give the pure compound **6a** (0.15 g, 78% yield) as a white solid, mp 148–150 °C. ^{1}H NMR (400 MHz, DMSO-d_6) δ 10.33 (s, 1H), 9.35 (s, 1H), 8.72 (s, 1H), 8.65 (s, 1H), 7.91 (s, 1H), 7.89–7.83 (m, 2H), 7.58 (dd, J = 9.7, 5.7 Hz, 3H), 7.47

https://dx.doi.org/10.1021/acs.jmedchem.0c02111
J. Med. Chem. XXXX, XXX, XXX–XXX

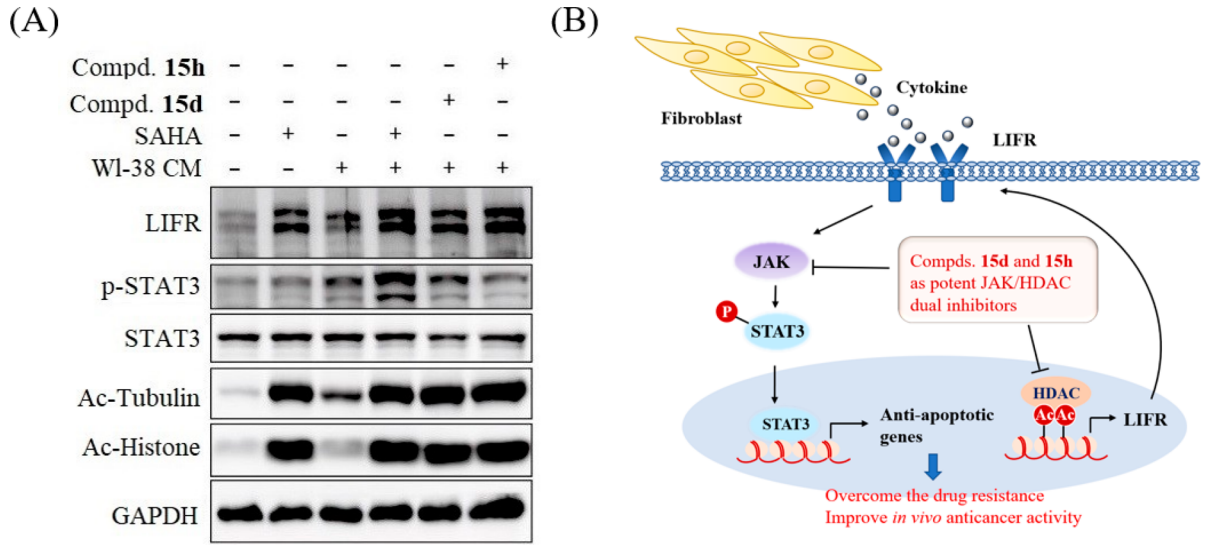

Figure 9. (A) Compounds **15d** and **15h** inhibited LIFR-JAK-STAT signaling in MDA-MB-231 stimulated by the conditioned medium (CM) of Wl-38 cells. The concentrations of compounds **15d**, **15h**, and SAHA were all 3 μM in this Western blot. (B) Compounds **15d** and **15h** could diminish the activation of LIFR-JAK-STAT signaling triggered by tumor-associated fibroblasts, which suggests that JAK/HDAC dual inhibitors could potentially overcome the drug resistance caused by the tumor microenvironment and improve the in vivo anticancer activity.

Table 6. In Vivo Antitumor Efficacy in MDA-MB-231 Xenograft Model

compd	administration	TGI (%)
SAHA	100 mg/kg/d, po	26
ruxolitinib	100 mg/kg/d, po	12
SAHA + ruxolitinib	100 + 100 mg/kg/d, po	33
15d	30 mg/kg/d, ip	37
15d	100 mg/kg/d, ip	49[a]

[a]Compared with the control group, the treated group showed statistically significant ($P < 0.05$) TGI by Student's two-tailed t test.

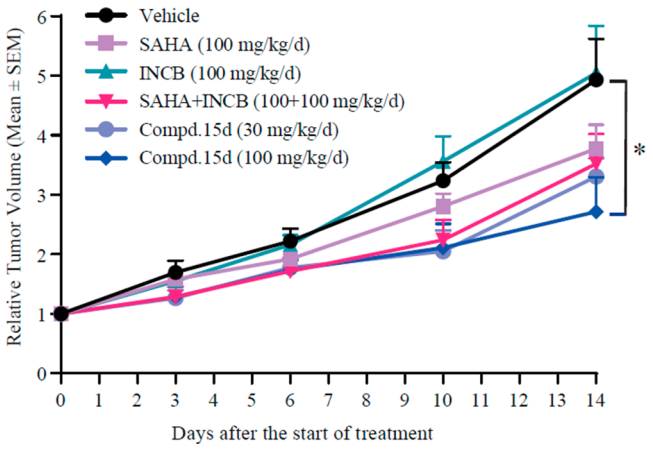

Figure 10. Growth curve of the implanted MDA-MB-231 xenograft in mice (RTV ± SEM). Ruxolitinib was indicated by INCB.

(s, 1H), 7.40 (t, J = 7.4 Hz, 1H), 6.62 (d, J = 3.7 Hz, 1H), 3.98 (t, J = 7.0 Hz, 2H), 1.91 (t, J = 7.3 Hz, 2H), 1.70 (p, J = 7.0 Hz, 2H), 1.44 (p, J = 7.3 Hz, 2H), 1.22 (h, J = 6.9, 6.4 Hz, 4H). ^{13}C NMR (101 MHz, DMSO-d_6) δ 169.5, 156.2, 152.2, 151.4, 137.9, 129.7, 126.8, 126.0, 123.8, 119.2, 112.2, 102.4, 51.9, 32.6, 30.2, 28.6, 26.2, 25.4. HRMS (AP-ESI) m/z calcd for $C_{22}H_{26}N_7O_2$ [M + H]$^+$ 420.2142, found 420.2151. Retention time: 7.6 min, eluted with 23% acetonitrile/77% water (containing 0.4% formic acid).

*7-(4-((7-(4-Bromophenyl)-7H-pyrrolo[2,3-d]pyrimidin-2-yl)-amino)-1H-pyrazol-1-yl)-N-hydroxyheptanamide (**6b**).* Ethyl 7-(4-((7-(4-bromophenyl)-7*H*-pyrrolo[2,3-*d*]pyrimidin-2-yl)amino)-1*H*-pyrazol-1-yl)heptanoate (**14b**, 0.10 g, 0.19 mmol) was reacted using a procedure similar to the synthesis of **6a**, affording compound **6b** (0.08 g, 83% yield) as a white solid, mp 182−184 °C. ^{1}H NMR (400 MHz, DMSO-d_6) δ 10.31 (s, 1H), 9.39 (s, 1H), 8.73 (d, J = 3.2 Hz, 1H), 8.65 (s, 1H), 7.96−7.69 (m, 5H), 7.58 (dd, J = 7.6, 3.8 Hz, 1H), 7.47 (d, J = 2.9 Hz, 1H), 6.65 (t, J = 3.5 Hz, 1H), 4.02 (t, J = 7.2 Hz, 2H), 2.03−1.87 (m, 2H), 1.72 (q, J = 7.2 Hz, 2H), 1.45 (p, J = 7.3 Hz, 2H), 1.39−1.12 (m, 4H). ^{13}C NMR (101 MHz, DMSO-d_6) δ 169.5, 156.6, 138.3, 137.2, 132.5, 129.6, 125.8, 125.6, 123.9, 119.2, 102.7, 51.9, 32.6, 30.3, 28.6, 26.3, 25.5. HRMS (AP-ESI) m/z calcd for $C_{22}H_{24}BrN_7O_2$ [M + H]$^+$ 498.1248, found 498.1248. Retention time: 28.7 min, eluted with 23% acetonitrile/77% water (containing 0.4% formic acid).

*7-(4-((7-(4-Chlorophenyl)-7H-pyrrolo[2,3-d]pyrimidin-2-yl)-amino)-1H-pyrazol-1-yl)-N-hydroxyheptanamide (**6c**).* Ethyl 7-(4-((7-(4-chlorophenyl)-7*H*-pyrrolo[2,3-*d*]pyrimidin-2-yl)amino)-1*H*-pyrazol-1-yl)heptanoate (**14c**, 0.08 g, 0.17 mmol) was reacted using a procedure similar to the synthesis of **6a**, affording compound **6c** (0.06 g, 77% yield) as a white solid, mp 185−187 °C. ^{1}H NMR (600 MHz, DMSO-d_6) δ 10.30 (s, 1H), 9.37 (s, 1H), 8.72 (s, 1H), 8.63 (s, 1H), 7.95−7.84 (m, 3H), 7.66−7.61 (m, 2H), 7.57 (d, J = 3.7 Hz, 1H), 7.46 (s, 1H), 6.64 (d, J = 3.7 Hz, 1H), 4.00 (t, J = 7.1 Hz, 2H), 1.90 (t, J = 7.4 Hz, 2H), 1.70 (p, J = 7.2 Hz, 2H), 1.44 (p, J = 7.4 Hz, 2H), 1.22 (p, J = 8.6 Hz, 4H). ^{13}C NMR (126 MHz, DMSO-d_6) δ 169.4, 156.4, 152.2, 151.8, 136.8, 130.9, 129.7, 129.6, 125.6, 125.3, 123.8, 119.2, 112.2, 102.7, 51.9, 32.6, 30.3, 28.6, 26.3, 25.5. HRMS (AP-ESI) m/z calcd for $C_{22}H_{25}ClN_7O_2$ [M + H]$^+$ 454.1753 found 454.1751. Retention time: 22.5 min, eluted with 23% acetonitrile/77% water (containing 0.4% formic acid).

*7-(4-((7-(4-Fluorophenyl)-7H-pyrrolo[2,3-d]pyrimidin-2-yl)-amino)-1H-pyrazol-1-yl)-N-hydroxyheptanamide (**6d**).* Ethyl 7-(4-((7-(4-fluorophenyl)-7*H*-pyrrolo[2,3-*d*]pyrimidin-2-yl)amino)-1*H*-pyrazol-1-yl)heptanoate (**14d**, 0.08 g, 0.17 mmol) was reacted using a procedure similar to the synthesis of **6a**, affording compound **6d** (0.06 g, 77% yield) as a white solid, mp 173−175 °C. ^{1}H NMR (600 MHz, DMSO-d_6) δ 10.30 (s, 1H), 9.35 (s, 1H), 8.72 (s, 1H), 8.63 (d, J = 1.8 Hz, 1H), 7.96−7.81 (m, 3H), 7.53 (d, J = 3.7 Hz, 1H), 7.49−7.38 (m, 3H), 6.62 (d, J = 3.7 Hz, 1H), 3.99 (t, J = 7.1 Hz, 2H), 1.89 (t, J = 7.4 Hz, 2H), 1.69 (t, J = 7.2 Hz, 2H), 1.43 (t, J = 7.3 Hz, 2H), 1.27−1.09 (m, 4H). ^{13}C NMR (126 MHz, DMSO-d_6) δ 169.5, 161.6, 159.7, 152.3, 134.2, 129.8, 126.0, 123.7, 119.3, 116.5, 116.3, 102.3, 51.8, 32.6, 30.2, 28.6, 26.2, 25.4. HRMS (AP-ESI) m/z calcd for

https://dx.doi.org/10.1021/acs.jmedchem.0c02111
J. Med. Chem. XXXX, XXX, XXX−XXX

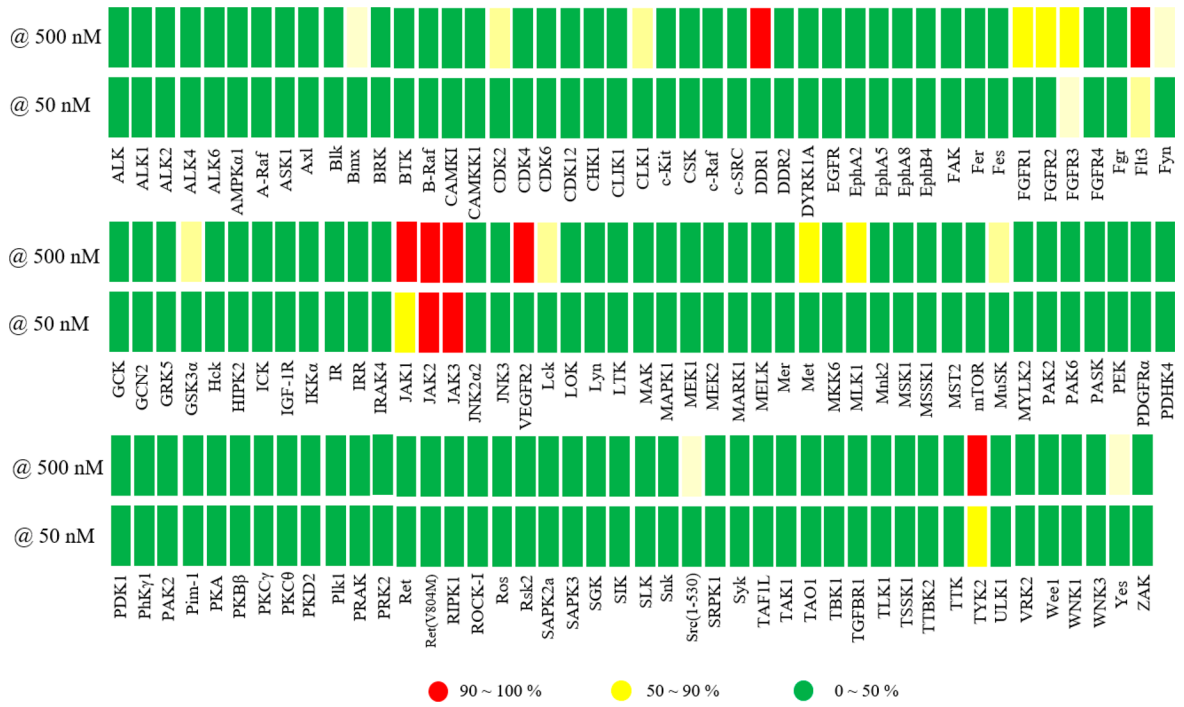

Figure 11. Kinome selectivity profiles for compound **15d**. Percent inhibition of phosphorylation of substrates at the indicated test compound concentration using a LANCE or HTRF detection method supplied by Eurofins Cerep Corporation. In these heat maps, inhibition <50% is assigned as green, inhibition >90% inhibition is assigned as red, and 50% < inhibition < 90% is assigned as yellow. In the kinome selectivity profiles, ATP concentration is close to the K_m of each tested kinase.

$C_{22}H_{25}FN_7O_2$ $[M + H]^+$ 438.2048, found 438.2055. Retention time: 9.4 min, eluted with 23% acetonitrile/77% water (containing 0.4% formic acid).

*7-(4-((7-(4-(Methylsulfonyl)phenyl)-7H-pyrrolo[2,3-d]pyrimidin-2-yl)amino)-1H-pyrazol-1-yl)-N-hydroxyheptanamide (**6e**).* Ethyl 7-(4-((7-(4-(methylsulfonyl)phenyl)-7*H*-pyrrolo[2,3-*d*]pyrimidin-2-yl)-amino)-1*H*-pyrazol-1-yl)heptanoate (**14e**, 0.10 g, 0.19 mmol) was reacted using a procedure similar to the synthesis of **6a**, affording compound **6e** (0.08 g, 83% yield) as a white solid, mp 198−200 °C. ^{1}H NMR (400 MHz, DMSO-d_6) δ 10.32 (s, 1H), 9.44 (s, 1H), 8.77 (s, 1H), 8.65 (s, 1H), 8.26 (d, J = 8.5 Hz, 2H), 8.12 (d, J = 8.5 Hz, 2H), 7.92 (s, 1H), 7.73 (d, J = 3.8 Hz, 1H), 7.53 (s, 1H), 6.72 (d, J = 3.8 Hz, 1H), 4.04 (t, J = 7.1 Hz, 2H), 3.30 (s, 3H), 1.91 (t, J = 7.4 Hz, 2H), 1.79−1.67 (m, 2H), 1.52−1.38 (m, 2H), 1.24 (d, J = 6.1 Hz, 4H). ^{13}C NMR (101 MHz, DMSO-d_6) δ 169.5, 156.7, 142.1, 129.9, 128.7, 123.7, 123.5, 51.9, 44.1, 32.6, 30.4, 28.6, 26.2, 25.5. HRMS (AP-ESI) m/z calcd for $C_{23}H_{27}N_7O_4S$ $[M + H]^+$ 498.1918, found 498.1917. Retention time: 8.5 min, eluted with 23% acetonitrile/77% water (containing 0.4% formic acid).

*6-(4-((7-(4-(Methylsulfonyl)phenyl)-7H-pyrrolo[2,3-d]pyrimidin-2-yl)amino)-1H-pyrazol-1-yl)-N-hydroxyhexanamide (**6f**).* Ethyl 6-(4-((7-(4-(methylsulfonyl)phenyl)-7*H*-pyrrolo[2,3-*d*]pyrimidin-2-yl)-amino)-1*H*-pyrazol-1-yl)hexanoate (**16f**, 0.10 g, 0.20 mmol) was reacted using a procedure similar to the synthesis of **6a**, affording compound **6f** (0.08 g, 83% yield) as a white solid, mp 208−210 °C. ^{1}H NMR (400 MHz, DMSO-d_6) δ 10.36 (s, 1H), 9.46 (s, 1H), 8.77 (s, 2H), 8.26 (d, J = 8.7 Hz, 2H), 8.13 (d, J = 8.6 Hz, 2H), 7.91 (s, 1H), 7.73 (d, J = 3.7 Hz, 1H), 7.54 (s, 1H), 6.73 (d, J = 3.8 Hz, 1H), 4.04 (t, J = 6.9 Hz, 2H), 3.37 (s, 3H), 1.92 (t, J = 7.3 Hz, 2H), 1.80−1.67 (m, 2H), 1.60−1.43 (m, 2H), 1.21 (dt, J = 15.1, 7.6 Hz, 2H). ^{13}C NMR (101 MHz, DMSO-d_6) δ 169.4, 156.7, 152.6, 152.2, 142.1, 138.1, 129.9, 128.7, 125.1, 123.8, 123.5, 119.5, 103.6, 51.8, 44.1, 32.5, 30.2, 26.1, 25.1. HRMS (AP-ESI) m/z calcd for $C_{22}H_{25}N_7O_4S$ $[M + H]^+$ 484.1761, found 484.1762. Retention time: 3.8 min, eluted with 23% acetonitrile/77% water (containing 0.4% formic acid).

*6-(4-((7-(4-Bromophenyl)-7H-pyrrolo[2,3-d]pyrimidin-2-yl)-amino)-1H-pyrazol-1-yl)-N-hydroxyhexanamide (**6g**).* Ethyl 6-(4-((7-(4-bromophenyl)-7*H*-pyrrolo[2,3-*d*]pyrimidin-2-yl) amino)-1*H*-pyrazol-1-yl)hexanoate (**14g**, 0.10 g, 0.20 mmol) was reacted using a procedure similar to the synthesis of **6a**, affording compound **6g** (0.09 g, 93% yield) as a white solid, mp 174−176 °C. ^{1}H NMR (600 MHz, DMSO-d_6) δ 10.30 (s, 1H), 9.37 (s, 1H), 8.72 (d, J = 3.0 Hz, 1H), 8.64 (s, 1H), 7.94−7.68 (m, 5H), 7.57 (dd, J = 7.6, 3.7 Hz, 1H), 7.47 (s, 1H), 6.63 (t, J = 3.5 Hz, 1H), 4.00 (t, J = 7.1 Hz, 2H), 1.91 (td, J = 7.5, 5.2 Hz, 2H), 1.71 (p, J = 7.2 Hz, 2H), 1.50 (h, J = 7.2 Hz, 2H), 1.25−1.13 (m, 2H). ^{13}C NMR (101 MHz, DMSO-d_6) δ 169.3, 156.6, 152.0, 138.3, 137.3, 132.5, 129.7, 125.8, 125.7, 123.9, 119.2, 119.1, 102.7, 51.8, 32.6, 30.2, 26.2, 25.2. HRMS (AP-ESI) m/z calcd for $C_{21}H_{22}BrN_7O_2$ $[M + H]^+$ 484.1091, found 484.1112. Retention time: 17.9 min, eluted with 23% acetonitrile/77% water (containing 0.4% formic acid).

*The Procedures for the Preparation of Compounds **8**, **9**, **10a,b**, and **11a,b** Were Described in Our Previous Paper.[31] General Procedure for the Preparation of **13a**−**13e**; 2-Chloro-7-phenyl-7H-pyrrolo[2,3-d]pyrimidine (**13a**).* To a solution of 2-chloro-7*H*-pyrrolo[2,3-*d*]pyrimidine (1.0 g, 6.51 mmol) and iodobenzene (2.66 g, 13.02 mmol) in dioxane (20 mL) was added CuI (0.5 g, 7.24 mmol), K_3PO_4 (2.0 g, 9.46 mmol), and *trans*-1,2-cyclohexanediamine (0.20 g, 1.94 mmol). The resulting mixture was irradiated in a microwave (150 W) at 130 °C for 1 h. The resulting mixture was filtered through Celite and concentrated under reduced pressure to give a residue, which was dissolved in DCM (300 mL). The organic layer was washed with water (100 mL) and brine (100 mL), dried over sodium sulfate, filtered, and concentrated to give the crude product, which was purified by silica gel chromatography (CH_2Cl_2/EtOAc, 20:1 V/V) to give compound **13a** (0.3 g, 20% yield) as a white solid. ^{1}H NMR (400 MHz, DMSO-d_6) δ 9.08 (s, 1H), 8.08 (d, J = 3.7 Hz, 1H), 7.87−7.79 (m, 2H), 7.69−7.59 (m, 2H), 7.49 (ddt, J = 7.9, 6.9, 1.1 Hz, 1H), 6.95 (d, J = 3.7 Hz, 1H). ESI-MS m/z = 230.1 $[M + H]^+$.

*7-(4-Bromophenyl)-2-chloro-7H-pyrrolo[2,3-d]pyrimidine (**13b**).* 2-Chloro-7*H*-pyrrolo[2,3-*d*]pyrimidine (0.5 g, 3.26 mmol) and 1-bromo-4-iodobenzene (0.65 g, 2.30 mmol) were reacted using a procedure similar to the synthesis of **13a**, affording compound **13b** (0.5 g, 50% yield) as a white solid. ^{1}H NMR (400 MHz, DMSO-d_6) δ

https://dx.doi.org/10.1021/acs.jmedchem.0c02111
J. Med. Chem. XXXX, XXX, XXX−XXX

9.10 (s, 1H), 8.20 (d, J = 3.8 Hz, 1H), 8.16 (s, 4H), 7.01 (d, J = 3.8 Hz, 1H), 3.31 (s, 3H). ESI-MS m/z = 308.2 $[M + H]^+$.

*2-Chloro-7-(4-chlorophenyl)-7H-pyrrolo[2,3-d]pyrimidine (**13c**).* 2-Chloro-7*H*-pyrrolo[2,3-*d*]pyrimidine (0.68 g, 4.43 mmol) and 1-chloro-4-iodobenzene (2.11 g, 8.86 mmol) were reacted using a procedure similar to the synthesis of **13a**, affording compound **13c** (0.45 g, 39% yield) as a white solid. ^{1}H NMR (400 MHz, DMSO-d_6) δ 9.04 (s, 1H), 8.05 (d, J = 3.7 Hz, 1H), 7.91−7.78 (m, 2H), 7.74−7.61 (m, 2H), 6.92 (d, J = 3.7 Hz, 1H). ESI-MS m/z = 265.1 $[M + H]^+$.

*2-Chloro-7-(4-fluorophenyl)-7H-pyrrolo[2,3-d]pyrimidine (**13d**).* 2-Chloro-7*H*-pyrrolo[2,3-*d*]pyrimidine (0.50 g, 3.26 mmol) and 1-fluoro-4-iodobenzene (1.45 g, 6.51 mmol) were reacted using a procedure similar to the synthesis of **13a**, affording compound **13d** (0.20 g, 25% yield) as a white solid. ^{1}H NMR (400 MHz, DMSO-d_6) δ 9.04 (s, 1H), 8.02 (d, J = 3.7 Hz, 1H), 7.87−7.77 (m, 2H), 7.50−7.39 (m, 2H), 6.91 (dd, J = 3.7, 0.7 Hz, 1H). ESI-MS m/z = 248.1 $[M + H]^+$.

*2-Chloro-7-(4-(methylsulfonyl)phenyl)-7H-pyrrolo[2,3-d]-pyrimidine (**13e**).* 2-Chloro-7*H*-pyrrolo[2,3-*d*]pyrimidine (0.5 g, 3.26 mmol) and 1-bromo-4-(methylsulfonyl)benzene (0.65 g, 2.66 mmol) were reacted using a procedure similar to the synthesis of **13a**, affording compound **13e** (0.5 g, 50% yield) as a white solid. ^{1}H NMR (400 MHz, DMSO-d_6) δ 9.10 (s, 1H), 8.20 (d, J = 3.8 Hz, 1H), 8.16 (s, 4H), 7.01 (d, J = 3.8 Hz, 1H), 3.31 (s, 3H). ESI-MS m/z = 308.2 $[M + H]^+$.

*General Procedure for the Preparation of **13f**−**13s**. 7-Benzyl-2-chloro-7H-pyrrolo[2,3-d]pyrimidine (**13f**).* To a solution of 2-chloro-7*H*-pyrrolo[2,3-*d*]pyrimidine (0.8 g, 5.22 mmol) and (bromomethyl)-benzene (0.97 g, 5.75 mmol) in acetonitrile (80 mL) was added K_2CO_3 (1.4 g, 10.44 mmol). The resulting mixture was heated at 40−50 °C for 5 h. The resulting mixture was filtered through Celite and concentrated under reduced pressure to give a residue, which was dissolved in DCM (150 mL). The organic layer was washed with citric acid (100 mL), water (100 mL), and brine (100 mL), dried over sodium sulfate, filtered, and concentrated to give the crude product, which was purified by silica gel chromatography (petroleum ether/EtOAc, 8:1 v/v) to give compound **13f** (1.0 g, 78% yield) as a white solid. ^{1}H NMR (400 MHz, DMSO-d_6) δ 8.96 (s, 1H), 7.75 (d, J = 3.6 Hz, 1H), 7.39−7.19 (m, 5H), 6.73 (d, J = 3.6 Hz, 1H), 5.45 (s, 2H). ESI-MS m/z = 244.1 $[M + H]^+$.

*2-Chloro-7-(2-fluorobenzyl)-7H-pyrrolo[2,3-d]pyrimidine (**13g**).* 2-Chloro-7*H*-pyrrolo[2,3-*d*]pyrimidine (0.5 g, 3.26 mmol) and 1-(bromomethyl)-2-fluorobenzene (0.70 g, 3.74 mmol) were reacted using a procedure similar to the synthesis of **13f**, affording compound **13g** (0.78 g, 92% yield) as a white solid. ^{1}H NMR (400 MHz, DMSO-d_6) δ 8.96 (s, 1H), 7.77−7.61 (m, 1H), 7.37 (td, J = 7.6, 1.8 Hz, 1H), 7.28−7.20 (m, 1H), 7.20−7.08 (m, 2H), 6.74 (d, J = 3.6 Hz, 1H), 5.49 (d, J = 13.4 Hz, 2H). ESI-MS m/z = 262.1 $[M + H]^+$.

*2-Chloro-7-(2-chlorobenzyl)-7H-pyrrolo[2,3-d]pyrimidine (**13h**).* 2-Chloro-7*H*-pyrrolo[2,3-*d*]pyrimidine (0.6 g, 3.91 mmol) and 1-(bromomethyl)-2-chlorobenzene (0.88 g, 4.30 mmol) were reacted using a procedure similar to the synthesis of **13f**, affording compound **13h** (0.87 g, 80% yield) as a white solid. ^{1}H NMR (400 MHz, DMSO-d_6) δ 8.96 (s, 1H), 7.65 (d, J = 3.6 Hz, 1H), 7.51 (dd, J = 7.9, 1.3 Hz, 1H), 7.30 (dtd, J = 29.3, 7.5, 1.5 Hz, 2H), 6.82 (dd, J = 7.7, 1.7 Hz, 1H), 6.75 (d, J = 3.7 Hz, 1H), 5.52 (s, 2H). ESI-MS m/z = 279.1 $[M + H]^+$.

*2-Chloro-7-(3-fluorobenzyl)-7H-pyrrolo[2,3-d]pyrimidine (**13i**).* 2-Chloro-7*H*-pyrrolo[2,3-*d*]pyrimidine (0.5 g, 3.26 mmol) and 1-(bromomethyl)-3-fluorobenzene (0.64 g, 2.78 mmol) were reacted using a procedure similar to the synthesis of **13f**, affording compound **13i** (0.80 g, 96% yield) as a white solid. ^{1}H NMR (400 MHz, DMSO-d_6) δ 8.96 (s, 1H), 7.77 (d, J = 3.6 Hz, 1H), 7.39 (td, J = 7.9, 6.0 Hz, 1H), 7.25−6.96 (m, 3H), 6.75 (d, J = 3.6 Hz, 1H), 5.48 (s, 2H). ESI-MS m/z = 262.2 $[M + H]^+$.

*2-Chloro-7-(3-chlorobenzyl)-7H-pyrrolo[2,3-d]pyrimidine (**13j**).* 2-Chloro-7*H*-pyrrolo[2,3-*d*]pyrimidine (0.5 g, 3.26 mmol) and 1-(bromomethyl)-3-chlorobenzene (0.73 g, 3.58 mmol) were reacted using a procedure similar to the synthesis of **13f**, affording compound **13j** (0.78 g, 86% yield) as a white solid. ^{1}H NMR (400 MHz, DMSO-d_6) δ 8.96 (s, 1H), 7.77 (d, J = 3.6 Hz, 1H), 7.41−7.31 (m, 3H), 7.16 (ddd, J = 5.5, 3.1, 1.8 Hz, 1H), 6.74 (d, J = 3.6 Hz, 1H), 5.46 (s, 2H). ESI-MS m/z = 279.2 $[M + H]^+$.

*2-Chloro-7-(3-methoxybenzyl)-7H-pyrrolo[2,3-d]pyrimidine (**13k**).* 2-Chloro-7*H*-pyrrolo[2,3-*d*]pyrimidine (0.5 g, 3.26 mmol) and 1-(chloromethyl)-3-methoxybenzene (0.56 g, 3.58 mmol) were reacted using a procedure similar to the synthesis of **13f**, affording compound **13k** (0.70 g, 78% yield) as a white solid. ESI-MS m/z = 273.9 $[M + H]^+$.

*2-Chloro-7-(4-fluorobenzyl)-7H-pyrrolo[2,3-d]pyrimidine (**13l**).* 2-Chloro-7*H*-pyrrolo[2,3-*d*]pyrimidine (0.5 g, 3.26 mmol) and 1-(bromomethyl)-4-fluorobenzene (0.64 g, 2.78 mmol) were reacted using a procedure similar to the synthesis of **13f**, affording compound **13l** (0.70 g, 82% yield) as a white solid. ^{1}H NMR (400 MHz, DMSO-d_6) δ 8.95 (s, 1H), 7.74 (d, J = 3.6 Hz, 1H), 7.37−7.28 (m, 2H), 7.22−7.13 (m, 2H), 6.73 (d, J = 3.6 Hz, 1H), 5.44 (s, 2H). ESI-MS m/z = 262.1 $[M + H]^+$.

*2-Chloro-7-(4-chlorobenzyl)-7H-pyrrolo[2,3-d]pyrimidine (**13m**).* 2-Chloro-7*H*-pyrrolo[2,3-*d*]pyrimidine (0.50 g, 3.26 mmol) and 1-(bromomethyl)-4-chlorobenzene (0.75 g, 3.27 mmol) were reacted using a procedure similar to the synthesis of **13f**, affording compound **13m** (0.70 g, 78% yield) as a white solid. ^{1}H NMR (400 MHz, DMSO-d_6) δ 8.96 (s, 1H), 7.75 (d, J = 3.6 Hz, 1H), 7.45−7.37 (m, 2H), 7.30−7.22 (m, 2H), 6.74 (d, J = 3.6 Hz, 1H), 5.45 (s, 2H). ESI-MS m/z = 278.2 $[M + H]^+$.

*2-Chloro-7-(4-methylbenzyl)-7H-pyrrolo[2,3-d]pyrimidine (**13n**).* 2-Chloro-7*H*-pyrrolo[2,3-*d*]pyrimidine (0.50 g, 3.26 mmol) and 1-(bromomethyl)-4-methylbenzene (0.60 g, 3.27 mmol) were reacted using a procedure similar to the synthesis of **13f**, affording compound **13n** (0.70 g, 83% yield) as a white solid. ^{1}H NMR (400 MHz, DMSO-d_6) δ 8.94 (s, 1H), 7.71 (d, J = 3.6 Hz, 1H), 7.15 (s, 4H), 6.71 (d, J = 3.6 Hz, 1H), 5.40 (s, 2H), 2.26 (s, 3H). ESI-MS m/z = 258.1 $[M + H]^+$.

*2-Chloro-7-(4-methoxybenzyl)-7H-pyrrolo[2,3-d]pyrimidine (**13o**).* 2-Chloro-7*H*-pyrrolo[2,3-*d*]pyrimidine (0.50 g, 3.26 mmol) and 1-(bromomethyl)-4-methoxybenzene (0.65 g, 3.27 mmol) were reacted using a procedure similar to the synthesis of **13f**, affording compound **13o** (0.70 g, 79% yield) as a white solid. ESI-MS m/z = 274.3 $[M + H]^+$.

*2-Chloro-7-phenethyl-7H-pyrrolo[2,3-d]pyrimidine (**13p**).* 2-Chloro-7*H*-pyrrolo[2,3-*d*]pyrimidine (0.50 g, 3.26 mmol) and (2-bromoethyl)benzene (0.60 g, 3.27 mmol) were reacted using a procedure similar to the synthesis of **13f**, affording compound **13p** (0.70 g, 83% yield) as a white solid. ^{1}H NMR (400 MHz, DMSO-d_6) δ 8.88 (s, 1H), 7.58 (d, J = 3.6 Hz, 1H), 7.28−7.08 (m, 5H), 6.62 (d, J = 3.6 Hz, 1H), 4.46 (dd, J = 7.7, 6.7 Hz, 2H), 3.11 (t, J = 7.2 Hz, 2H). ESI-MS m/z = 258.1 $[M + H]^+$.

*2-Chloro-7-cyclopentyl-7H-pyrrolo[2,3-d]pyrimidine (**13q**).* 2-Chloro-7*H*-pyrrolo[2,3-*d*]pyrimidine (0.7 g, 4.56 mmol) and bromocyclopentane (1.36 g, 9.12 mmol) were reacted using a procedure similar to the synthesis of **13f**, affording compound **13q** (0.70 g, 69% yield) as a white solid. ^{1}H NMR (400 MHz, DMSO-d_6) δ 8.91 (s, 1H), 7.79 (d, J = 3.7 Hz, 1H), 6.71 (d, J = 3.7 Hz, 1H), 5.12−5.04 (m, 1H), 2.14 (ddt, J = 10.9, 5.3, 2.8 Hz, 2H), 1.93−1.83 (m, 4H), 1.76−1.67 (m, 2H). ESI-MS m/z = 222.3 $[M + H]^+$.

*2-Chloro-7-(cyclopropylmethyl)-7H-pyrrolo[2,3-d]pyrimidine (**13r**).* 2-Chloro-7*H*-pyrrolo[2,3-*d*]pyrimidine (1.0 g, 6.51 mmol) and (bromomethyl)cyclopropane (1.05 g, 7.81 mmol) were reacted using a procedure similar to the synthesis of **13f**, affording compound **13r** (0.90 g, 67% yield) as a white solid. ^{1}H NMR (400 MHz, DMSO-d_6) δ 8.92 (s, 1H), 7.76 (d, J = 3.6 Hz, 1H), 6.69 (d, J = 3.6 Hz, 1H), 4.08 (d, J = 7.2 Hz, 2H), 1.31−1.22 (m, 1H), 0.51 (dt, J = 8.0, 3.0 Hz, 2H), 0.47−0.38 (m, 2H). ESI-MS m/z = 208.2 $[M + H]^+$.

*2-Chloro-7-(cyclohexylmethyl)-7H-pyrrolo[2,3-d]pyrimidine (**13s**).* 2-Chloro-7*H*-pyrrolo[2,3-*d*]pyrimidine (1.0 g, 6.51 mmol) and (bromomethyl)cyclohexane (1.38 g, 7.81 mmol) were reacted using a procedure similar to the synthesis of **13f**, affording compound **13s** (1.20 g, 74% yield) as a white solid. ^{1}H NMR (400 MHz, DMSO-d_6) δ 8.92 (s, 1H), 7.67 (d, J = 3.5 Hz, 1H), 6.69 (d, J = 3.5 Hz, 1H), 4.06

https://dx.doi.org/10.1021/acs.jmedchem.0c02111
J. Med. Chem. XXXX, XXX, XXX−XXX

(d, J = 7.4 Hz, 2H), 1.85 (dqd, J = 11.1, 7.5, 3.8 Hz, 1H), 1.65 (h, J = 4.2, 3.4 Hz, 2H), 1.59 (s, 1H), 1.48−1.43 (m, 2H), 1.20−1.10 (m, 3H), 0.97 (qd, J = 11.5, 3.5 Hz, 2H). ESI-MS m/z = 250.1 $[M + H]^+$.

General Procedure for the Preparation of ***14a−14z*** *and* ***14A−14F****. Ethyl 7-(4-((7-Phenyl-7H-pyrrolo[2,3-d]pyrimidin-2-yl)amino)-1H-pyrazol-1-yl)heptanoate (****14a****).* 2-Chloro-7-phenyl-7*H*-pyrrolo[2,3-*d*]pyrimidine (**13a**, 0.23 g, 1.00 mmol) and ethyl 7-(4-amino-1*H*-pyrazol-1-yl)heptanoate (hydrochloride) (**11b**, 0.20 g, 0.83 mmol) were suspended in ethanol (16 mL). The mixture was irradiated in a microwave (150 W) at 125 °C for 2−3 h. Evaporation of the solvent under reduced pressure gave a residue, which was preliminarily purified by silica gel chromatography ($CH_2Cl_2/CH_3OH/Et_3N$, 100:1:0.25 v/v/v) to give the product **14a** (0.10 g, yield 27%) as a white solid. ESI-MS m/z = 433.2 $[M + H]^+$.

*Ethyl 7-(4-((7-(4-Bromophenyl)-7H-pyrrolo[2,3-d]pyrimidin-2-yl)amino)-1H-pyrazol-1-yl)heptanoate (****14b****).* 7-(4-Bromophenyl)-2-chloro-7*H*-pyrrolo[2,3-*d*]pyrimidine (**13b**, 0.3 g, 0.97 mmol) and ethyl 7-(4-amino-1*H*-pyrazol-1-yl)heptanoate (hydrochloride) (**11b**, 0.25 g, 0.91 mmol) were reacted using a procedure similar to the synthesis of **14a**, affording compound **14b** (0.10 g, yield 22%) as a white solid. ESI-MS m/z = 511.2 $[M + H]^+$.

*Ethyl 7-(4-((7-(4-Chlorophenyl)-7H-pyrrolo[2,3-d]pyrimidin-2-yl)amino)-1H-pyrazol-1-yl)heptanoate (****14c****).* 2-Chloro-7-(4-chlorophenyl)-7*H*-pyrrolo[2,3-*d*]pyrimidine (**13c**, 0.26 g, 1.00 mmol) and ethyl 7-(4-amino-1*H*-pyrazol-1-yl)heptanoate (hydrochloride) (**11b**, 0.20 g, 0.83 mmol) were reacted using a procedure similar to the synthesis of **14a**, affording compound **14c** (0.08 g, yield 20%) as a white solid. ESI-MS m/z = 467.1 $[M + H]^+$.

*Ethyl 7-(4-((7-(4-Fluorophenyl)-7H-pyrrolo[2,3-d]pyrimidin-2-yl)amino)-1H-pyrazol-1-yl)heptanoate (****14d****).* 2-Chloro-7-(4-fluorophenyl)-7*H*-pyrrolo[2,3-*d*]pyrimidine (**13d**, 0.22 g, 0.90 mmol) and ethyl 7-(4-amino-1*H*-pyrazol-1-yl)heptanoate (hydrochloride) (**11b**, 0.18 g, 0.75 mmol) were reacted using a procedure similar to the synthesis of **14a**, affording compound **14d** (0.08 g, yield 20%) as a white solid. ESI-MS m/z = 451.2 $[M + H]^+$.

*Ethyl 7-(4-((7-(4-(Methylsulfonyl)phenyl)-7H-pyrrolo[2,3-d]-pyrimidin-2-yl) amino)-1H-pyrazol-1-yl)heptanoate (****14e****).* 2-Chloro-7-(4-(methylsulfonyl)phenyl)-7*H*-pyrrolo[2,3-*d*]pyrimidine (**13e**, 0.30 g, 0.97 mmol) and ethyl 7-(4-amino-1*H*-pyrazol-1-yl)heptanoate (hydrochloride) (**11b**, 0.25 g, 0.91 mmol) were reacted using a procedure similar to the synthesis of **14a**, affording compound **14e** (0.10 g, yield 20%) as a white solid. ESI-MS m/z = 511.1 $[M + H]^+$.

*Ethyl 6-(4-((7-(4-(Methylsulfonyl)phenyl)-7H-pyrrolo[2,3-d]-pyrimidin-2-yl) amino)-1H-pyrazol-1-yl)hexanoate (****14f****).* 2-Chloro-7-(4-(methylsulfonyl)phenyl)-7*H*-pyrrolo[2,3-*d*]pyrimidine (**13e**, 0.30 g, 0.97 mmol) and ethyl 6-(4-amino-1*H*-pyrazol-1-yl)hexanoate (hydrochloride) (**11a**, 0.25 g, 0.95 mmol) were reacted using a procedure similar to the synthesis of **14a**, affording compound **14f** (0.10 g, 22% yield) as a white solid. ^{1}H NMR (400 MHz, DMSO-d_6) δ 9.45 (s, 1H), 8.77 (s, 1H), 8.25 (d, J = 8.8 Hz, 2H), 8.12 (d, J = 8.6 Hz, 2H), 7.92 (s, 1H), 7.73 (d, J = 3.8 Hz, 1H), 7.52 (s, 1H), 6.72 (d, J = 3.8 Hz, 1H), 4.04 (q, J = 6.3, 5.7 Hz, 2H), 3.95 (t, J = 6.6 Hz, 2H), 3.30 (s, 3H), 2.25 (t, J = 7.3 Hz, 2H), 1.80−1.68 (m, 2H), 1.52−1.47 (m, 2H), 1.26−1.21 (m, 2H), 0.84 (t, J = 7.4 Hz, 3H). ESI-MS m/z = 497.2 $[M + H]^+$.

*Ethyl 6-(4-((7-(4-Bromophenyl)-7H-pyrrolo[2,3-d]pyrimidin-2-yl)amino)-1H-pyrazol-1-yl)hexanoate (****14g****).* 7-(4-Bromophenyl)-2-chloro-7*H*-pyrrolo[2,3-*d*]pyrimidine (**13b**, 0.3 g, 0.97 mmol) and ethyl 6-(4-amino-1*H*-pyrazol-1-yl)hexanoate (hydrochloride) (**11a**, 0.25 g, 0.95 mmol) were reacted using a procedure similar to the synthesis of **14a**, affording compound **14g** (0.15 g, 32% yield) as a white solid. ESI-MS m/z = 497.1 $[M + H]^+$.

*Ethyl 6-(4-((7-Benzyl-7H-pyrrolo[2,3-d]pyrimidin-2-yl)amino)-1H-pyrazol-1-yl)hexanoate (****14h****).* 7-Benzyl-2-chloro-7*H*-pyrrolo[2,3-*d*]pyrimidine (**13f**, 0.35 g, 1.44 mmol) and ethyl 6-(4-amino-1*H*-pyrazol-1-yl)hexanoate (hydrochloride) (**11a**, 0.25 g, 0.95 mmol) were reacted using a procedure similar to the synthesis of **14a**, affording compound **14h** (0.18 g, 45% yield) as a white solid. ^{1}H NMR (400 MHz, DMSO-d_6) δ 9.23 (s, 1H), 8.63 (s, 1H), 8.02−7.84 (m, 1H), 7.49 (d, J = 0.9 Hz, 1H), 7.30 (dtd, J = 12.0, 8.3, 7.7, 5.8 Hz, 6H), 6.43 (d, J = 3.5 Hz, 1H), 5.38 (s, 2H), 4.02 (tt, J = 7.1, 3.8 Hz, 4H), 2.23 (dt, J = 14.6, 7.3 Hz, 2H), 1.71 (h, J = 8.3, 7.7 Hz, 2H), 1.60−1.43 (m, 2H), 1.28−1.17 (m, 2H), 1.15 (d, J = 6.9 Hz, 3H). ESI-MS m/z = 433.2 $[M + H]^+$.

*Ethyl 7-(4-((7-Benzyl-7H-pyrrolo[2,3-d]pyrimidin-2-yl)amino)-1H-pyrazol-1-yl)heptanoate (****14i****).* 7-Benzyl-2-chloro-7*H*-pyrrolo[2,3-*d*]pyrimidine (**13f**, 0.35 g, 1.44 mmol) and ethyl 7-(4-amino-1*H*-pyrazol-1-yl)heptanoate (hydrochloride) (**11b**, 0.25 g, 0.91 mmol) were reacted using a procedure similar to the synthesis of **14a**, affording compound **14i** (0.15 g, yield 38%) as a white solid. ^{1}H NMR (400 MHz, DMSO-d_6) δ 9.23 (s, 1H), 8.63 (s, 1H), 7.93 (s, 1H), 7.48 (s, 1H), 7.34−7.22 (m, 6H), 6.43 (d, J = 3.5 Hz, 1H), 5.38 (s, 2H), 4.10−3.95 (m, 4H), 2.29−2.16 (m, 2H), 1.71 (p, J = 7.0 Hz, 2H), 1.48 (pd, J = 7.2, 2.4 Hz, 2H), 1.26 (ddd, J = 23.4, 11.8, 7.5 Hz, 4H), 1.18−1.05 (m, 3H). ESI-MS m/z = 447.1 $[M + H]^+$.

*Ethyl 6-(4-((7-(2-Fluorobenzyl)-7H-pyrrolo[2,3-d]pyrimidin-2-yl)amino)-1H-pyrazol-1-yl)hexanoate (****14j****).* 2-Chloro-7-(2-fluorobenzyl)-7*H*-pyrrolo[2,3-*d*]pyrimidine (**13g**, 0.35 g, 1.34 mmol) and ethyl 6-(4-amino-1*H*-pyrazol-1-yl)hexanoate (hydrochloride) (**11a**, 0.25 g, 0.95 mmol) were reacted using a procedure similar to the synthesis of **14a**, affording compound **14j** (0.15 g, 35% yield) as a white solid. ESI-MS m/z = 451.1 $[M + H]^+$.

*Ethyl 7-(4-((7-(2-Fluorobenzyl)-7H-pyrrolo[2,3-d]pyrimidin-2-yl)amino)-1H-pyrazol-1-yl)heptanoate (****14k****).* 2-Chloro-7-(2-fluorobenzyl)-7*H*-pyrrolo[2,3-*d*]pyrimidine (**13g**, 0.35 g, 1.34 mmol) and ethyl 7-(4-amino-1*H*-pyrazol-1-yl)heptanoate (hydrochloride) (**11b**, 0.25 g, 0.91 mmol) were reacted using a procedure similar to the synthesis of **14a**, affording compound **14k** (0.16 g, yield 38%) as a white solid. ^{1}H NMR (600 MHz, DMSO-d_6) δ 9.73 (s, 1H), 8.73 (s, 1H), 7.98 (s, 1H), 7.54 (s, 1H), 7.42 (d, J = 3.7 Hz, 1H), 7.39−7.34 (m, 1H), 7.25 (dd, J = 10.4, 8.2 Hz, 1H), 7.19 (t, J = 7.4 Hz, 1H), 7.14 (t, J = 7.4 Hz, 1H), 6.58 (d, J = 3.7 Hz, 1H), 5.46 (s, 2H), 4.07−4.00 (m, 4H), 2.24 (t, J = 7.4 Hz, 2H), 1.78−1.69 (m, 2H), 1.48 (q, J = 7.5 Hz, 2H), 1.25 (dq, J = 26.2, 7.8 Hz, 4H), 1.15 (t, J = 7.1 Hz, 3H). ESI-MS m/z = 465.1 $[M + H]^+$.

*Ethyl 6-(4-((7-(2-Chlorobenzyl)-7H-pyrrolo[2,3-d]pyrimidin-2-yl)amino)-1H-pyrazol-1-yl)hexanoate (****14l****).* 2-Chloro-7-(2-chlorobenzyl)-7*H*-pyrrolo[2,3-*d*]pyrimidine (**13h**, 0.37 g, 1.33 mmol) and ethyl 6-(4-amino-1*H*-pyrazol-1-yl)hexanoate (hydrochloride) (**11a**, 0.25 g, 0.95 mmol) were reacted using a procedure similar to the synthesis of **14a**, affording compound **14l** (0.15 g, 30% yield) as a white solid. ESI-MS m/z = 467.2 $[M + H]^+$.

*Ethyl 7-(4-((7-(2-Chlorobenzyl)-7H-pyrrolo[2,3-d]pyrimidin-2-yl)amino)-1H-pyrazol-1-yl)heptanoate (****14m****).* 2-Chloro-7-(2-chlorobenzyl)-7*H*-pyrrolo[2,3-*d*]pyrimidine (**13h**, 0.35 g, 1.25 mmol) and ethyl 7-(4-amino-1*H*-pyrazol-1-yl)heptanoate (hydrochloride) (**11b**, 0.25 g, 0.91 mmol) were reacted using a procedure similar to the synthesis of **14a**, affording compound **14m** (0.10 g, yield 20%) as a white solid. ESI-MS m/z = 481.2 $[M + H]^+$.

*Ethyl 6-(4-((7-(3-Fluorobenzyl)-7H-pyrrolo[2,3-d]pyrimidin-2-yl)amino)-1H-pyrazol-1-yl)hexanoate (****14n****).* 2-Chloro-7-(3-fluorobenzyl)-7*H*-pyrrolo[2,3-*d*]pyrimidine (**13i**, 0.35 g, 1.34 mmol) and ethyl 6-(4-amino-1*H*-pyrazol-1-yl)hexanoate (hydrochloride) (**11a**, 0.25 g, 0.95 mmol) were reacted using a procedure similar to the synthesis of **14a**, affording compound **14n** (0.15 g, yield 35%) as a white solid. ESI-MS m/z = 451.1 $[M + H]^+$.

*Ethyl 7-(4-((7-(3-Fluorobenzyl)-7H-pyrrolo[2,3-d]pyrimidin-2-yl)amino)-1H-pyrazol-1-yl)heptanoate (****14o****).* 2-Chloro-7-(3-fluorobenzyl)-7*H*-pyrrolo[2,3-*d*]pyrimidine (**13i**, 0.35 g, 1.34 mmol) and ethyl 7-(4-amino-1*H*-pyrazol-1-yl)heptanoate (hydrochloride) (**11b**, 0.25 g, 0.91 mmol) were reacted using a procedure similar to the synthesis of **14a**, affording compound **14o** (0.16 g, yield 38%) as a white solid. ESI-MS m/z = 465.1 $[M + H]^+$.

*Ethyl 6-(4-((7-(3-Chlorobenzyl)-7H-pyrrolo[2,3-d]pyrimidin-2-yl)amino)-1H-pyrazol-1-yl)hexanoate (****14p****).* 2-Chloro-7-(3-chlorobenzyl)-7*H*-pyrrolo[2,3-*d*]pyrimidine (**13j**, 0.37 g, 1.34 mmol) and ethyl 6-(4-amino-1*H*-pyrazol-1-yl)hexanoate (hydrochloride) (**11a**, 0.25 g, 0.95 mmol) were reacted using a procedure similar to the synthesis of **14a**, affording compound **14p** (0.10 g, yield 20%) as a white solid. ESI-MS m/z = 467.2 $[M + H]^+$.

https://dx.doi.org/10.1021/acs.jmedchem.0c02111
J. Med. Chem. XXXX, XXX, XXX−XXX

*Ethyl 7-(4-((7-(3-Chlorobenzyl)-7H-pyrrolo[2,3-d]pyrimidin-2-yl)-amino)-1H-pyrazol-1-yl)heptanoate (**14q**).* 2-Chloro-7-(3-chlorobenzyl)-7*H*-pyrrolo[2,3-*d*]pyrimidine (**13j**, 0.37 g, 1.34 mmol) and ethyl 7-(4-amino-1*H*-pyrazol-1-yl)heptanoate (hydrochloride) (**11b**, 0.25 g, 0.91 mmol) were reacted using a procedure similar to the synthesis of **14a**, affording compound **14q** (0.10 g, yield 20%) as a white solid. ESI-MS m/z = 481.1 $[M + H]^+$.

*Ethyl 6-(4-((7-(3-Methoxybenzyl)-7H-pyrrolo[2,3-d]pyrimidin-2-yl)amino)-1H-pyrazol-1-yl)hexanoate (**14r**).* 2-Chloro-7-(3-methoxybenzyl)-7*H*-pyrrolo[2,3-*d*]pyrimidine (**13k**, 0.37 g, 1.34 mmol) and ethyl 6-(4-amino-1*H*-pyrazol-1-yl)hexanoate (hydrochloride) (**11a**, 0.25 g, 0.95 mmol) were reacted using a procedure similar to the synthesis of **14a**, affording compound **14r** (0.12 g, yield 27%) as a white solid. ESI-MS m/z = 463.2 $[M + H]^+$.

*Ethyl 7-(4-((7-(3-Methoxybenzyl)-7H-pyrrolo[2,3-d]pyrimidin-2-yl)amino)-1H-pyrazol-1-yl)heptanoate (**14s**).* 2-Chloro-7-(3-methoxybenzyl)-7*H*-pyrrolo[2,3-*d*]pyrimidine (**13k**, 0.29 g, 1.09 mmol) and ethyl 7-(4-amino-1*H*-pyrazol-1-yl)heptanoate (hydrochloride) (**11b**, 0.25 g, 0.91 mmol) were reacted using a procedure similar to the synthesis of **14a**, affording compound **14s** (0.10 g, yield 20%) as a white solid. ESI-MS m/z = 477.3 $[M + H]^+$.

*Ethyl 6-(4-((7-(4-Fluorobenzyl)-7H-pyrrolo[2,3-d]pyrimidin-2-yl)-amino)-1H-pyrazol-1-yl)hexanoate (**14t**).* 2-Chloro-7-(4-fluorobenzyl)-7*H*-pyrrolo[2,3-*d*]pyrimidine (**13l**, 0.35 g, 1.34 mmol) and ethyl 6-(4-amino-1*H*-pyrazol-1-yl)hexanoate (hydrochloride) (**11a**, 0.25 g, 0.95 mmol) were reacted using a procedure similar to the synthesis of **14a**, affording compound **14t** (0.15 g, 35% yield) as a white solid. ESI-MS m/z = 451.2 $[M + H]^+$.

*Ethyl 7-(4-((7-(4-Fluorobenzyl)-7H-pyrrolo[2,3-d]pyrimidin-2-yl)-amino)-1H-pyrazol-1-yl)heptanoate (**14u**).* 2-Chloro-7-(4-fluorobenzyl)-7*H*-pyrrolo[2,3-*d*]pyrimidine (**13l**, 0.35 g, 1.34 mmol) and ethyl 7-(4-amino-1*H*-pyrazol-1-yl)heptanoate (hydrochloride) (**11b**, 0.25 g, 0.91 mmol) were reacted using a procedure similar to the synthesis of **14a**, affording compound **14u** (0.16 g, yield 38%) as a white solid. ESI-MS m/z = 465.2 $[M + H]^+$.

*Ethyl 6-(4-((7-(4-Chlorobenzyl)-7H-pyrrolo[2,3-d]pyrimidin-2-yl)-amino)-1H-pyrazol-1-yl)hexanoate (**14v**).* 2-Chloro-7-(4-chlorobenzyl)-7*H*-pyrrolo[2,3-*d*]pyrimidine (**13m**, 0.35 g, 1.25 mmol) and ethyl 6-(4-amino-1*H*-pyrazol-1-yl)hexanoate (hydrochloride) (**11a**, 0.25 g, 0.95 mmol) were reacted using a procedure similar to the synthesis of **14a**, affording compound **14v** (0.15 g, 34% yield) as a white solid. ESI-MS m/z = 467.1 $[M + H]^+$.

*Ethyl 7-(4-((7-(4-Chlorobenzyl)-7H-pyrrolo[2,3-d]pyrimidin-2-yl)-amino)-1H-pyrazol-1-yl)heptanoate (**14w**).* 2-Chloro-7-(4-chlorobenzyl)-7*H*-pyrrolo[2,3-*d*]pyrimidine (**13m**, 0.35 g, 1.25 mmol) and ethyl 7-(4-amino-1*H*-pyrazol-1-yl)heptanoate (hydrochloride) (**11b**, 0.25 g, 0.91 mmol) were reacted using a procedure similar to the synthesis of **14a**, affording compound **14w** (0.15 g, yield 34%) as a white solid. ESI-MS m/z = 481.1 $[M + H]^+$.

*Ethyl 6-(4-((7-(4-Methylbenzyl)-7H-pyrrolo[2,3-d]pyrimidin-2-yl)-amino)-1H-pyrazol-1-yl)hexanoate (**14x**).* 2-Chloro-7-(4-methylbenzyl)-7*H*-pyrrolo[2,3-*d*]pyrimidine (**13n**, 0.35 g, 1.36 mmol) and ethyl 6-(4-amino-1*H*-pyrazol-1-yl)hexanoate (hydrochloride) (**11a**, 0.25 g, 0.95 mmol) were reacted using a procedure similar to the synthesis of **14a**, affording compound **14x** (0.20 g, 47% yield) as a white solid. ESI-MS m/z = 447.2 $[M + H]^+$.

*Ethyl 7-(4-((7-(4-Methylbenzyl)-7H-pyrrolo[2,3-d]pyrimidin-2-yl)-amino)-1H-pyrazol-1-yl)heptanoate (**14y**).* 2-Chloro-7-(4-methylbenzyl)-7*H*-pyrrolo[2,3-*d*]pyrimidine (**13n**, 0.35 g, 1.36 mmol) and ethyl 7-(4-amino-1*H*-pyrazol-1-yl)heptanoate (hydrochloride) (**11b**, 0.25 g, 0.91 mmol) were reacted using a procedure similar to the synthesis of **14a**, affording compound **14y** (0.20 g, yield 47%) as a white solid. ESI-MS m/z = 461.1 $[M + H]^+$.

*Ethyl 6-(4-((7-(4-Methoxybenzyl)-7H-pyrrolo[2,3-d]pyrimidin-2-yl)amino)-1H-pyrazol-1-yl)hexanoate (**14z**).* 2-Chloro-7-(4-methoxybenzyl)-7*H*-pyrrolo[2,3-*d*]pyrimidine (**13o**, 0.35 g, 1.28 mmol) and ethyl 6-(4-amino-1*H*-pyrazol-1-yl)hexanoate (hydrochloride) (**11a**, 0.25 g, 0.95 mmol) were reacted using a procedure similar to the synthesis of **14a**, affording compound **14z** (0.18 g, 41% yield) as a white solid. ^{1}H NMR (400 MHz, DMSO-d_6) δ 9.23 (s, 1H), 8.61 (s, 1H), 8.04−7.95 (m, 1H), 7.51 (t, J = 0.7 Hz, 1H), 7.31−7.20 (m, 3H), 6.98−6.82 (m, 2H), 6.40 (d, J = 3.5 Hz, 1H), 5.30 (s, 2H), 4.09−3.95 (m, 4H), 3.70 (s, 3H), 2.23 (dt, J = 14.5, 7.4 Hz, 2H), 1.80−1.68 (m, 2H), 1.53 (td, J = 7.8, 3.0 Hz, 2H), 1.30−1.18 (m, 2H), 1.13 (d, J = 6.3 Hz, 3H). ESI-MS m/z = 463.1 $[M + H]^+$.

*Ethyl 7-(4-((7-(4-Methoxybenzyl)-7H-pyrrolo[2,3-d]pyrimidin-2-yl)amino)-1H-pyrazol-1-yl)heptanoate (**14A**).* 2-Chloro-7-(4-methoxybenzyl)-7*H*-pyrrolo[2,3-*d*]pyrimidine (**13o**, 0.35 g, 1.28 mmol) and ethyl 7-(4-amino-1*H*-pyrazol-1-yl)heptanoate (hydrochloride) (**11b**, 0.25 g, 0.91 mmol) were reacted using a procedure similar to the synthesis of **14a**, affording compound **14A** (0.18 g, yield 41%) as a white solid. ESI-MS m/z = 477.1 $[M + H]^+$.

*Ethyl 6-(4-((7-Phenethyl-7H-pyrrolo[2,3-d]pyrimidin-2-yl)-amino)-1H-pyrazol-1-yl)hexanoate (**14B**).* 2-Chloro-7-phenethyl-7*H*-pyrrolo[2,3-*d*]pyrimidine (**13p**, 0.35 g, 1.36 mmol) and ethyl 6-(4-amino-1*H*-pyrazol-1-yl)hexanoate (hydrochloride) (**11a**, 0.25 g, 0.95 mmol) were reacted using a procedure similar to the synthesis of **14a**, affording compound **14B** (0.16 g, yield 38%) as a white solid. ESI-MS m/z = 447.2 $[M + H]^+$.

*Ethyl 7-(4-((7-Phenethyl-7H-pyrrolo[2,3-d]pyrimidin-2-yl)-amino)-1H-pyrazol-1-yl)heptanoate (**14C**).* 2-Chloro-7-phenethyl-7*H*-pyrrolo[2,3-*d*]pyrimidine (**13p**, 0.35 g, 1.36 mmol) and ethyl 7-(4-amino-1*H*-pyrazol-1-yl)heptanoate (hydrochloride) (**11b**, 0.25 g, 0.91 mmol) were reacted using a procedure similar to the synthesis of **14a**, affording compound **14C** (0.16 g, yield 38%) as a white solid. ESI-MS m/z = 461.2 $[M + H]^+$.

*Ethyl 7-(4-((7-Cyclopentyl-7H-pyrrolo[2,3-d]pyrimidin-2-yl)-amino)-1H-pyrazol-1-yl)heptanoate (**14D**).* 2-Chloro-7-cyclopentyl-7*H*-pyrrolo[2,3-*d*]pyrimidine (**13q**, 0.30 g, 1.35 mmol) and ethyl 7-(4-amino-1*H*-pyrazol-1-yl)heptanoate (hydrochloride) (**11b**, 0.25 g, 0.91 mmol) were reacted using a procedure similar to the synthesis of **14a**, affording compound **14D** (0.12 g, yield 21%) as a colorless oil. ESI-MS m/z = 425.2 $[M + H]^+$.

*Ethyl 7-(4-((7-(Cyclopropylmethyl)-7H-pyrrolo[2,3-d]pyrimidin-2-yl)amino)-1H-pyrazol-1-yl)heptanoate (**14E**).* 2-Chloro-7-(cyclopropylmethyl)-7*H*-pyrrolo[2,3-*d*]pyrimidine (**13r**, 0.28 g, 1.35 mmol) and ethyl 7-(4-amino-1*H*-pyrazol-1-yl)heptanoate (hydrochloride) (**11b**, 0.25 g, 0.91 mmol) were reacted using a procedure similar to the synthesis of **14a**, affording compound **14E** (0.10 g, 18% yield) as a colorless oil. ESI-MS m/z = 425.2 $[M + H]^+$.

*Ethyl 7-(4-((7-(Cyclohexylmethyl)-7H-pyrrolo[2,3-d]pyrimidin-2-yl)amino)-1H-pyrazol-1-yl)heptanoate (**14F**).* 2-Chloro-7-(cyclohexylmethyl)-7*H*-pyrrolo[2,3-*d*]pyrimidine (**13s**, 0.32 g, 1.35 mmol) and ethyl 7-(4-amino-1*H*-pyrazol-1-yl)heptanoate (hydrochloride) (**11b**, 0.25 g, 0.91 mmol) were reacted using a procedure similar to the synthesis of **14a**, affording compound **14F** (0.15 g, 25% yield) as a white solid. ESI-MS m/z = 453.3 $[M + H]^+$.

*General Procedure for the Preparation of **15a−l**, **16a−j**, and **17a−c**. 6-(4-((7-Benzyl-7H-pyrrolo[2,3-d]pyrimidin-2-yl)amino)-1H-pyrazol-1-yl)-N-hydroxyhexanamide (**15a**).* Ethyl 6-(4-((7-benzyl-7*H*-pyrrolo[2,3-*d*]pyrimidin-2-yl)amino)-1*H*-pyrazol-1-yl) hexanoate (**14h**, 0.16 g, 0.37 mmol) was reacted using a procedure similar to the synthesis of **6a**, affording compound **15a** (0.12 g, 80% yield) as a white solid, mp 160−162 °C. ^{1}H NMR (400 MHz, DMSO-d_6) δ 10.39 (s, 1H), 9.24 (s, 1H), 8.70 (s, 1H), 8.63 (s, 1H), 7.92 (s, 1H), 7.50 (s, 1H), 7.29 (td, J = 12.0, 9.8, 5.7 Hz, 6H), 6.43 (d, J = 3.6 Hz, 1H), 5.39 (s, 2H), 4.02 (t, J = 6.9 Hz, 2H), 1.93 (t, J = 7.3 Hz, 2H), 1.72 (p, J = 7.2 Hz, 2H), 1.50 (p, J = 7.5 Hz, 2H), 1.20 (p, J = 7.7 Hz, 2H). ^{13}C NMR (101 MHz, DMSO-d_6) δ 169.4, 156.3, 152.3, 151.1, 138.6, 129.6, 129.0, 127.8, 127.5, 126.8, 124.2, 119.1, 111.5, 100.1, 51.6, 47.5, 32.6, 30.2, 26.1, 25.2. HRMS (AP-ESI) m/z calcd for $C_{22}H_{25}N_7O_2$ $[M + H]^+$ 420.2142, found 420.2147. Retention time: 3.7 min, eluted with 23% acetonitrile/77% water (containing 0.4% formic acid).

*7-(4-((7-Benzyl-7H-pyrrolo[2,3-d]pyrimidin-2-yl)amino)-1H-pyrazol-1-yl)-N-hydroxyheptanamide (**15b**).* Ethyl 7-(4-((7-benzyl-7*H*-pyrrolo[2,3-*d*]pyrimidin-2-yl)amino)-1*H*-pyrazol-1-yl) heptanoate (**14i**, 0.12 g, 0.26 mmol) was reacted using a procedure similar to the synthesis of **6a**, affording compound **15b** (0.12 g, 95% yield) as a white solid, mp 150−152 °C. ^{1}H NMR (400 MHz, DMSO-d_6) δ 10.35 (s, 1H) 9.23 (s, 1H), 8.67 (d, J = 1.8 Hz, 1H), 8.63 (s, 1H), 7.97−7.88 (m, 1H), 7.48 (d, J = 0.7 Hz, 1H), 7.36−7.22 (m, 6H),

https://dx.doi.org/10.1021/acs.jmedchem.0c02111
J. Med. Chem. XXXX, XXX, XXX−XXX

6.43 (d, J = 3.6 Hz, 1H), 5.38 (s, 2H), 4.02 (t, J = 7.0 Hz, 2H), 1.92 (t, J = 7.3 Hz, 2H), 1.71 (q, J = 7.1 Hz, 2H), 1.44 (q, J = 7.2 Hz, 2H), 1.22 (d, J = 6.8 Hz, 4H). ^{13}C NMR (101 MHz, DMSO-d_6) δ 169.5, 156.3, 151.1, 138.6, 129.6, 129.0, 127.8, 127.5, 124.2, 119.1, 100.2, 51.7, 47.4, 32.6, 30.4, 28.6, 26.2, 25.4. ESI-MS m/z = 434 $[M + H]^+$. HRMS (AP-ESI) m/z calcd for $C_{23}H_{27}N_7O_2$ $[M + H]^+$ 434.2299, found 434.2304. Retention time: 5.5 min, eluted with 23% acetonitrile/77% water (containing 0.4% formic acid).

*6-(4-((7-(2-Fluorobenzyl)-7H-pyrrolo[2,3-d]pyrimidin-2-yl)-amino)-1H-pyrazol-1-yl)-N-hydroxyhexanamide (**15c**).* Ethyl 6-(4-((7-(2-fluorobenzyl)-7*H*-pyrrolo[2,3-*d*]pyrimidin-2-yl) amino)-1*H*-pyrazol-1-yl)hexanoate (**14j**, 0.12 g, 0.26 mmol) was reacted using a procedure similar to the synthesis of **6a**, affording compound **15c** (0.08 g, 73% yield) as a white solid, mp 156−158 °C. ^{1}H NMR (400 MHz, DMSO-d_6) δ 10.36 (s, 1H), 9.23 (s, 1H), 8.76 (s, 1H), 8.63 (s, 1H), 7.94 (s, 1H), 7.48 (s, 1H), 7.34 (dtd, J = 8.7, 5.6, 2.7 Hz, 1H), 7.29−7.21 (m, 2H), 7.12 (d, J = 6.2 Hz, 2H), 6.45 (d, J = 3.5 Hz, 1H), 5.44 (s, 2H), 4.02 (t, J = 7.0 Hz, 2H), 1.93 (t, J = 7.4 Hz, 2H), 1.80−1.63 (m, 2H), 1.59−1.41 (m, 2H), 1.21 (tt, J = 9.6, 6.3 Hz, 2H). ^{13}C NMR (101 MHz, DMSO-d_6) δ 169.4, 161.4, 159.0, 156.3, 152.3, 151.2, 130.1, 130.1, 129.8, 129.6, 126.7, 125.2, 125.1, 125.1, 124.2, 119.1, 115.9, 115.7, 111.4, 100.4, 51.7, 41.3, 32.6, 30.2, 26.1, 25.2. HRMS (AP-ESI) m/z calcd for $C_{22}H_{24}FN_7O_2$ $[M + H]^+$ 438.2048, found 438.2053. Retention time: 4.6 min, eluted with 23% acetonitrile/77% water (containing 0.4% formic acid).

*7-(4-((7-(2-Fluorobenzyl)-7H-pyrrolo[2,3-d]pyrimidin-2-yl)-amino)-1H-pyrazol-1-yl)-N-hydroxyheptanamide (**15d**).* Ethyl 7-(4-((7-(2-fluorobenzyl)-7*H*-pyrrolo[2,3-*d*]pyrimidin-2-yl) amino)-1*H*-pyrazol-1-yl)heptanoate (**14k**, 0.15 g, 0.32 mmol) was reacted using a procedure similar to the synthesis of **6a**, affording compound **15d** (0.10 g, 70% yield) as a white solid, mp 158−160 °C. ^{1}H NMR (600 MHz, DMSO-d_6) δ 10.31 (s, 1H), 9.22 (s, 1H), 8.63 (d, J = 16.2 Hz, 2H), 7.92 (s, 1H), 7.45 (s, 1H), 7.35−7.29 (m, 1H), 7.26−7.19 (m, 2H), 7.13−7.04 (m, 2H), 6.43 (d, J = 3.6 Hz, 1H), 5.42 (s, 2H), 4.00 (t, J = 7.0 Hz, 2H), 1.90 (t, J = 7.4 Hz, 2H), 1.70 (t, J = 7.2 Hz, 2H), 1.49−1.37 (m, 2H), 1.21 (q, J = 12.7, 8.3 Hz, 4H). ^{13}C NMR (101 MHz, DMSO-d_6) δ 169.5, 161.4, 159.0, 156.3, 152.3, 151.2, 130.1, 130.1, 129.8, 129.6, 126.7, 125.2, 125.1, 125.0, 124.2, 119.1, 115.9, 115.7, 111.4, 100.4, 51.7, 41.3, 32.6, 30.4, 28.6, 26.2, 25.5. HRMS (AP-ESI) m/z calcd for $C_{23}H_{26}FN_7O_2$ $[M + H]^+$ 452.2205, found 452.2209. Retention time: 6.2 min, eluted with 25% acetonitrile/75% water (containing 0.4% formic acid).

*6-(4-((7-(2-Chlorobenzyl)-7H-pyrrolo[2,3-d]pyrimidin-2-yl)-amino)-1H-pyrazol-1-yl)-N-hydroxyhexanamide (**15e**).* Ethyl 6-(4-((7-(2-chlorobenzyl)-7*H*-pyrrolo[2,3-*d*]pyrimidin-2-yl)amino)-1*H*-pyrazol-1-yl)hexanoate (**14l**, 0.12 g, 0.25 mmol) was reacted using a procedure similar to the synthesis of **6a**, affording compound **15e** (0.08 g, 68% yield) as a white solid, mp 172−174 °C. ^{1}H NMR (600 MHz, DMSO-d_6) δ 10.35 (s, 1H), 9.25 (s, 1H), 8.67 (s, 2H), 7.82 (s, 1H), 7.54 (dd, J = 8.0, 1.3 Hz, 1H), 7.43 (s, 1H), 7.33 (td, J = 7.7, 1.8 Hz, 1H), 7.27−7.23 (m, 2H), 6.79 (s, 1H), 6.49 (d, J = 3.6 Hz, 1H), 5.48 (s, 2H), 3.97 (t, J = 7.0 Hz, 2H), 1.92 (t, J = 7.4 Hz, 2H), 1.69 (p, J = 7.4 Hz, 2H), 1.49 (p, J = 7.4 Hz, 2H), 1.18 (p, J = 7.7 Hz, 2H). ^{13}C NMR (126 MHz, DMSO-d_6) δ 169.4, 156.3, 151.2, 135.7, 131.9, 129.8, 129.6, 128.7, 128.0, 126.8, 124.2, 100.4, 51.7, 45.2, 32.6, 30.2, 26.1, 25.1. HRMS (AP-ESI) m/z calcd for $C_{22}H_{25}ClN_7O_2$ $[M + H]^+$ 454.1753, found 454.1749. Retention time: 8.7 min, eluted with 23% acetonitrile/77% water (containing 0.4% formic acid).

*7-(4-((7-(2-Chlorobenzyl)-7H-pyrrolo[2,3-d]pyrimidin-2-yl)-amino)-1H-pyrazol-1-yl)-N-hydroxyheptanamide (**15f**).* Ethyl 7-(4-((7-(2-chlorobenzyl)-7*H*-pyrrolo[2,3-*d*]pyrimidin-2-yl)amino)-1*H*-pyrazol-1-yl)heptanoate (**14m**, 0.10 g, 0.20 mmol) was reacted using a procedure similar to the synthesis of **6a**, affording compound **15f** (0.08 g, 82% yield) as a white solid, mp 168−170 °C. ^{1}H NMR (600 MHz, DMSO-d_6) δ 10.35 (s, 1H), 9.25 (s, 1H), 8.71−8.64 (m, 2H), 7.83 (s, 1H), 7.54 (dd, J = 8.0, 1.2 Hz, 1H), 7.42 (s, 1H), 7.33 (td, J = 7.7, 1.7 Hz, 1H), 7.27−7.22 (m, 2H), 6.78 (d, J = 7.7 Hz, 1H), 6.49 (d, J = 3.6 Hz, 1H), 5.48 (s, 2H), 3.98 (t, J = 7.0 Hz, 2H), 1.92 (t, J = 7.4 Hz, 2H), 1.68 (p, J = 7.2 Hz, 2H), 1.45 (p, J = 7.4 Hz, 2H), 1.22 (dp, J = 22.3, 7.4 Hz, 4H). ^{13}C NMR (124 MHz, DMSO-d_6) δ 169.5, 156.3, 152.5, 151.2, 131.9, 129.8, 129.6, 128.7, 128.0, 126.8, 124.2, 118.9, 100.5, 51.8, 45.2, 32.6, 30.4, 28.6, 26.2, 25.4. HRMS (AP-ESI) m/z calcd for $C_{23}H_{27}ClN_7O_2$ $[M + H]^+$ 468.1909, found 468.1900. Retention time: 11.7 min, eluted with 23% acetonitrile/77% water (containing 0.4% formic acid).

*6-(4-((7-(3-Fluorobenzyl)-7H-pyrrolo[2,3-d]pyrimidin-2-yl)-amino)-1H-pyrazol-1-yl)-N-hydroxyhexanamide (**15g**).* Ethyl 6-(4-((7-(3-fluorobenzyl)-7*H*-pyrrolo[2,3-*d*]pyrimidin-2-yl)amino)-1*H*-pyrazol-1-yl)hexanoate (**14n**, 0.16 g, 0.35 mmol) was reacted using a procedure similar to the synthesis of **6a**, affording compound **15g** (0.10 g, 67% yield) as a white solid, mp 156−158 °C. ^{1}H NMR (400 MHz, DMSO-d_6) δ 10.35 (s, 1H), 9.23 (s, 1H), 8.64 (s, 2H), 7.91 (s, 1H), 7.48 (s, 1H), 7.41−7.33 (m, 1H), 7.31 (d, J = 3.6 Hz, 1H), 7.14−7.04 (m, 3H), 6.45 (d, J = 3.6 Hz, 1H), 5.41 (s, 2H), 4.02 (t, J = 7.0 Hz, 2H), 1.92 (t, J = 7.4 Hz, 2H), 1.72 (p, J = 7.2 Hz, 2H), 1.49 (h, J = 7.2 Hz, 2H), 1.29−1.12 (m, 2H). ^{13}C NMR (101 MHz, DMSO-d_6) δ 169.4, 163.8, 161.4, 156.3, 152.3, 151.2, 141.6, 141.5, 131.1, 131.0, 129.6, 126.7, 124.2, 123.5, 123.5, 119.1, 114.7, 114.5, 114.4, 114.2, 100.3, 51.6, 46.9, 32.6, 30.2, 26.1, 25.1. HRMS (AP-ESI) m/z calcd for $C_{22}H_{24}FN_7O_2$ $[M + H]^+$ 438.2048, found 438.2049. Retention time: 4.7 min, eluted with 23% acetonitrile/77% water (containing 0.4% formic acid).

*7-(4-((7-(3-Fluorobenzyl)-7H-pyrrolo[2,3-d]pyrimidin-2-yl)-amino)-1H-pyrazol-1-yl)-N-hydroxyheptanamide (**15h**).* Ethyl 7-(4-((7-(3-fluorobenzyl)-7*H*-pyrrolo[2,3-*d*]pyrimidin-2-yl) amino)-1*H*-pyrazol-1-yl)heptanoate (**14o**, 0.15 g, 0.32 mmol) was reacted using a procedure similar to the synthesis of **6a**, affording compound **15h** (0.10 g, 70% yield) as a white solid, mp 158−160 °C. ^{1}H NMR (400 MHz, DMSO-d_6) δ 10.33 (s, 1H), 9.23 (s, 1H), 8.63 (s, 2H), 7.91 (s, 1H), 7.47 (s, 1H), 7.41−7.32 (m, 1H), 7.30 (d, J = 3.6 Hz, 1H), 7.13−7.06 (m, 3H), 6.44 (d, J = 3.6 Hz, 1H), 5.40 (s, 2H), 4.02 (t, J = 7.0 Hz, 2H), 1.92 (t, J = 7.4 Hz, 2H), 1.71 (t, J = 7.1 Hz, 2H), 1.51−1.40 (m, 2H), 1.21 (dd, J = 8.1, 4.5 Hz, 4H). ^{13}C NMR (101 MHz, DMSO-d_6) δ 169.5, 163.8, 161.4, 156.3, 152.3, 151.2, 141.6, 141.5, 131.1, 131.0, 129.6, 126.7, 124.1, 123.5, 123.5, 119.1, 114.7, 114.5, 114.4, 114.2, 100.3, 51.7, 46.9, 32.6, 30.4, 28.6, 26.2, 25.4. HRMS (AP-ESI) m/z calcd for $C_{23}H_{26}FN_7O_2$ $[M + H]^+$ 452.2205, found 452.2205. Retention time:6.7 min, eluted with 23% acetonitrile/77% water (containing 0.4% formic acid).

*6-(4-((7-(3-Chlorobenzyl)-7H-pyrrolo[2,3-d]pyrimidin-2-yl)-amino)-1H-pyrazol-1-yl)-N-hydroxyhexanamide (**15i**).* Ethyl 6-(4-((7-(3-fluorobenzyl)-7*H*-pyrrolo[2,3-*d*]pyrimidin-2-yl)amino)-1*H*-pyrazol-1-yl)hexanoate (**14p**, 0.06 g, 0.13 mmol) was reacted using a procedure similar to the synthesis of **6a**, affording compound **15i** (0.05 g, 86% yield) as a white solid, mp 160−162 °C. ^{1}H NMR (400 MHz, DMSO-d_6) δ 10.32 (s, 1H), 9.46 (s, 1H), 9.23 (s, 1H), 8.64 (s, 1H), 8.62 (s, 1H), 7.89 (s, 1H), 7.46 (s, 1H), 7.36−7.29 (m, 3H), 7.20 (dd, J = 6.8, 2.1 Hz, 1H), 6.43 (d, J = 3.6 Hz, 1H), 5.38 (s, 2H), 4.00 (t, J = 7.0 Hz, 2H), 1.90 (t, J = 7.4 Hz, 2H), 1.76−1.63 (m, 2H), 1.54−1.43 (m, 2H), 1.19 (q, J = 7.8 Hz, 2H). ^{13}C NMR (126 MHz, DMSO-d_6) δ 169.4, 141.0, 133.6, 131.0, 129.8, 127.8, 127.4, 126.2, 123.8, 119.4, 111.5, 100.6, 51.7, 46.9, 32.6, 30.2, 26.1, 25.1. HRMS (AP-ESI) m/z calcd for $C_{22}H_{25}ClN_7O_2$ $[M + H]^+$ 454.1753, found 454.1755. Retention time: 8.2 min, eluted with 23% acetonitrile/77% water (containing 0.4% formic acid).

*7-(4-((7-(3-Chlorobenzyl)-7H-pyrrolo[2,3-d]pyrimidin-2-yl)-amino)-1H-pyrazol-1-yl)-N-hydroxyheptanamide (**15j**).* Ethyl 7-(4-((7-(3-chlorobenzyl)-7*H*-pyrrolo[2,3-*d*]pyrimidin-2-yl)amino)-1*H*-pyrazol-1-yl)heptanoate (**14q**, 0.09 g, 0.18 mmol) was reacted using a procedure similar to the synthesis of **6a**, affording compound **15j** (0.08 g, 91% yield) as a white solid, mp 150−152 °C. ^{1}H NMR (600 MHz, DMSO-d_6) δ 10.33 (s, 1H), 9.24 (s, 1H), 8.63 (d, J = 12.3 Hz, 2H), 7.90 (s, 1H), 7.46 (s, 1H), 7.35−7.27 (m, 4H), 7.19 (d, J = 7.0 Hz, 1H), 6.43 (d, J = 3.5 Hz, 1H), 5.38 (s, 2H), 4.00 (t, J = 7.0 Hz, 2H), 1.89 (t, J = 7.4 Hz, 2H), 1.69 (t, J = 7.1 Hz, 2H), 1.43 (t, J = 7.3 Hz, 2H), 1.20 (h, J = 7.3 Hz, 4H). ^{13}C NMR (126 MHz, DMSO-d_6) δ 169.4, 140.8, 133.6, 131.0, 127.9, 127.5, 126.3, 51.8, 47.0, 32.6, 30.3, 28.6, 26.2, 25.4. HRMS (AP-ESI) m/z calcd for $C_{23}H_{27}ClN_7O_2$ $[M + H]^+$ 468.1909, found 468.1917. Retention time: 11.3 min, eluted with 23% acetonitrile/77% water (containing 0.4% formic acid).

https://dx.doi.org/10.1021/acs.jmedchem.0c02111
J. Med. Chem. XXXX, XXX, XXX−XXX

*N-Hydroxy-6-(4-((7-(3-methoxybenzyl)-7H-pyrrolo[2,3-d]-pyrimidin-2-yl)amino)-1H-pyrazol-1-yl)hexanamide (**15k**).* Ethyl 6-(4-((7-(3-methoxybenzyl)-7*H*-pyrrolo[2,3-*d*]pyrimidin-2-yl)amino)-1*H*-pyrazol-1-yl)hexanoate (**14r**, 0.10 g, 0.21 mmol) was reacted using a procedure similar to the synthesis of **6a**, affording compound **15k** (0.07 g, 72% yield) as a white solid, mp 148−150 °C. ^{1}H NMR (600 MHz, DMSO-d_6) δ 10.34 (s, 1H), 9.27 (s, 1H), 8.64 (s, 2H), 7.93 (s, 1H), 7.51 (s, 1H), 7.30 (d, J = 3.6 Hz, 1H), 7.24 (t, J = 7.9 Hz, 1H), 6.88 (s, 1H), 6.83 (dt, J = 8.3, 2.5 Hz, 2H), 6.44 (d, J = 3.6 Hz, 1H), 5.35 (s, 2H), 4.02 (t, J = 7.0 Hz, 2H), 3.68 (s, 3H), 1.92 (t, J = 7.4 Hz, 2H), 1.78−1.68 (m, 2H), 1.55−1.46 (m, 2H), 1.29−1.14 (m, 2H). ^{13}C NMR (126 MHz, DMSO-d_6) δ 169.4, 159.8, 140.1, 130.1, 129.7, 119.7, 119.2, 113.6, 112.9, 100.2, 55.4, 51.6, 47.4, 32.6, 30.2, 26.1, 25.1. HRMS (AP-ESI) m/z calcd for $C_{23}H_{28}N_7O_3$ [M + H]$^+$ 450.2248, found 450.2259. Retention time: 4.4 min, eluted with 23% acetonitrile/77% water (containing 0.4% formic acid).

*N-Hydroxy-7-(4-((7-(3-methoxybenzyl)-7H-pyrrolo[2,3-d]-pyrimidin-2-yl)amino)-1H-pyrazol-1-yl)heptanamide (**15l**).* Ethyl 7-(4-((7-(3-methoxybenzyl)-7*H*-pyrrolo[2,3-*d*]pyrimidin-2-yl)amino)-1*H*-pyrazol-1-yl)heptanoate (**14s**, 0.09 g, 0.18 mmol) was reacted using a procedure similar to the synthesis of **6a**, affording compound **15l** (0.07 g, 80% yield) as a white solid, mp 145−147 °C. ^{1}H NMR (400 MHz, DMSO-d_6) δ 10.31 (s, 1H), 9.22 (s, 1H), 8.62 (d, J = 20.4 Hz, 2H), 7.91 (s, 1H), 7.48 (s, 1H), 7.31−7.15 (m, 2H), 6.93−6.70 (m, 3H), 6.52−6.31 (m, 1H), 5.32 (s, 2H), 3.99 (d, J = 7.2 Hz, 2H), 3.66 (s, 3H), 1.90 (t, J = 7.3 Hz, 2H), 1.69 (t, J = 7.7 Hz, 2H), 1.53−1.38 (m, 2H), 1.20 (s, 4H). ^{13}C NMR (126 MHz, DMSO-d_6) δ 169.5, 159.8, 152.3, 140.1, 130.1, 129.7, 119.7, 119.2, 113.6, 112.9, 100.3, 55.4, 51.7, 47.4, 32.6, 30.4, 28.6, 26.2, 25.4. HRMS (AP-ESI) m/z calcd for $C_{24}H_{30}N_7O_3$ [M + H]$^+$ 464.2405, found 464.2405. Retention time: 5.8 min, eluted with 23% acetonitrile/77% water (containing 0.4% formic acid).

*6-(4-((7-(4-Fluorobenzyl)-7H-pyrrolo[2,3-d]pyrimidin-2-yl)-amino)-1H-pyrazol-1-yl)-N-hydroxyhexanamide (**16a**).* Ethyl 6-(4-((7-(4-fluorobenzyl)-7*H*-pyrrolo[2,3-*d*]pyrimidin-2-yl) amino)-1*H*-pyrazol-1-yl)hexanoate (**14t**, 0.12 g, 0.26 mmol) was reacted using a procedure similar to the synthesis of **6a**, affording compound **16a** (0.08 g, 73% yield) as a white solid, mp 176−178 °C. ^{1}H NMR (400 MHz, DMSO-d_6) δ 10.34 (s, 1H), 9.22 (s, 1H), 8.64 (d, J = 12.3 Hz, 2H), 7.92 (s, 1H), 7.50 (s, 1H), 7.40−7.29 (m, 2H), 7.27 (d, J = 3.6 Hz, 1H), 7.20−7.09 (m, 2H), 6.42 (d, J = 3.6 Hz, 1H), 5.37 (s, 2H), 4.02 (t, J = 7.0 Hz, 2H), 1.92 (t, J = 7.4 Hz, 2H), 1.72 (t, J = 7.5 Hz, 2H), 1.49 (q, J = 7.5 Hz, 2H), 1.30−1.14 (m, 2H). ^{13}C NMR (101 MHz, DMSO-d_6) δ 169.4, 163.1, 160.6, 156.3, 152.2, 151.1, 134.8, 134.8, 129.7, 129.7, 129.6, 126.6, 124.2, 119.1, 115.9, 115.7, 111.5, 100.3, 51.6, 46.7, 32.6, 30.2, 26.1, 25.1. HRMS (AP-ESI) m/z calcd for $C_{22}H_{24}FN_7O_2$ [M + H]$^+$ 438.2048, found 438.2043. Retention time: 5.1 min, eluted with 23% acetonitrile/77% water (containing 0.4% formic acid).

*7-(4-((7-(4-Fluorobenzyl)-7H-pyrrolo[2,3-d]pyrimidin-2-yl)-amino)-1H-pyrazol-1-yl)-N-hydroxyheptanamide (**16b**).* Ethyl 7-(4-((7-(4-fluorobenzyl)-7*H*-pyrrolo[2,3-*d*]pyrimidin-2-yl) amino)-1*H*-pyrazol-1-yl)heptanoate (**14u**, 0.15 g, 0.32 mmol) was reacted using a procedure similar to the synthesis of **6a**, affording compound **16b** (0.12 g, 83% yield) as a white solid, mp 160−162 °C. ^{1}H NMR (400 MHz, DMSO-d_6) δ 10.34 (s, 1H), 9.22 (s, 1H), 8.63 (s, 2H), 7.91 (s, 1H), 7.50 (s, 1H), 7.37−7.30 (m, 2H), 7.26 (d, J = 3.6 Hz, 1H), 7.15 (t, J = 8.9 Hz, 2H), 6.42 (d, J = 3.5 Hz, 1H), 5.37 (s, 2H), 4.02 (t, J = 7.0 Hz, 2H), 1.92 (t, J = 7.4 Hz, 2H), 1.71 (t, J = 7.1 Hz, 2H), 1.50−1.41 (m, 2H), 1.28−1.19 (m, 4H). ^{13}C NMR (101 MHz, DMSO-d_6) δ 169.5, 160.6, 156.3, 152.2, 151.1, 134.8, 134.8, 129.7, 129.6, 126.6, 124.2, 119.1, 115.9, 115.7, 100.3, 51.7, 46.7, 32.6, 30.4, 28.6, 26.2, 25.4. ESI-MS m/z = 452 [M + H]$^+$. HRMS (AP-ESI) m/z calcd for $C_{23}H_{26}FN_7O_2$ [M + H]$^+$ 452.2202, found 452.2201. Retention time: 7.5 min, eluted with 23% acetonitrile/77% water (containing 0.4% formic acid).

*6-(4-((7-(4-Chlorobenzyl)-7H-pyrrolo[2,3-d]pyrimidin-2-yl)-amino)-1H-pyrazol-1-yl)-N-hydroxyhexanamide (**16c**).* Ethyl 6-(4-((7-(4-chlorobenzyl)-7*H*-pyrrolo[2,3-*d*]pyrimidin-2-yl)amino)-1*H*-pyrazol-1-yl)hexanoate (**14v**, 0.15 g, 0.32 mmol) was reacted using a procedure similar to the synthesis of **6a**, affording compound **16c** (0.10 g, 70% yield) as a white solid, mp 158−160 °C. ^{1}H NMR (400 MHz, DMSO-d_6) δ 10.34 (s, 1H), 9.23 (s, 1H), 8.65 (d, J = 10.2 Hz, 2H), 7.88 (s, 1H), 7.49 (s, 1H), 7.44−7.35 (m, 2H), 7.28 (dd, J = 6.1, 2.5 Hz, 3H), 6.44 (d, J = 3.6 Hz, 1H), 5.39 (s, 2H), 4.02 (t, J = 7.0 Hz, 2H), 1.93 (t, J = 7.4 Hz, 2H), 1.72 (p, J = 7.2 Hz, 2H), 1.51 (p, J = 7.5 Hz, 2H), 1.20 (qd, J = 9.3, 8.7, 6.1 Hz, 2H). ^{13}C NMR (101 MHz, DMSO-d_6) δ 169.4, 156.3, 152.3, 151.2, 137.6, 132.4, 129.6, 129.4, 129.0, 126.7, 124.2, 119.1, 100.3, 51.6, 46.8, 32.6, 30.2, 26.1, 25.2. HRMS (AP-ESI) m/z calcd for $C_{22}H_{24}ClN_7O_2$ [M + H]$^+$ 454.1753, found 454.1757. Retention time: 9.6 min, eluted with 23% acetonitrile/77% water (containing 0.4% formic acid).

*7-(4-((7-(4-Chlorobenzyl)-7H-pyrrolo[2,3-d]pyrimidin-2-yl)-amino)-1H-pyrazol-1-yl)-N-hydroxyheptanamide (**16d**).* Ethyl 7-(4-((7-(4-chlorobenzyl)-7*H*-pyrrolo[2,3-*d*]pyrimidin-2-yl)amino)-1*H*-pyrazol-1-yl)heptanoate (**14w**, 0.15 g, 0.31 mmol) was reacted using a procedure similar to the synthesis of **6a**, affording compound **16d** (0.10 g, 70% yield) as a white solid, mp 174−176 °C. ^{1}H NMR (600 MHz, DMSO-d_6) δ 10.33 (s, 1H), 9.27 (s, 1H), 8.63 (s, 2H), 7.87 (s, 1H), 7.47 (d, J = 3.0 Hz, 1H), 7.39−7.24 (m, 5H), 6.44 (d, J = 3.6 Hz, 1H), 5.37 (s, 2H), 4.01 (t, J = 7.0 Hz, 2H), 1.91 (t, J = 7.4 Hz, 2H), 1.69 (p, J = 7.1 Hz, 2H), 1.45 (p, J = 7.3 Hz, 2H), 1.31−1.18 (m, 4H). ^{13}C NMR (101 MHz, DMSO-d_6) δ 169.5, 156.3, 152.3, 151.2, 137.6, 132.4, 129.6, 129.3, 129.0, 126.7, 124.2, 119.1, 111.5, 100.3, 51.7, 46.8, 32.6, 30.4, 28.6, 26.2, 25.4. ESI-MS m/z = 468 [M + H]$^+$. HRMS (AP-ESI) m/z calcd for $C_{23}H_{26}ClN_7O_2$ [M + H]$^+$ 468.1909, found 468.1905. Retention time: 15.6 min, eluted with 23% acetonitrile/77% water (containing 0.4% formic acid).

*6-(4-((7-(4-Methylbenzyl)-7H-pyrrolo[2,3-d]pyrimidin-2-yl)-amino)-1H-pyrazol-1-yl)-N-hydroxyhexanamide (**16e**).* Ethyl 6-(4-((7-(4-methylbenzyl)-7*H*-pyrrolo[2,3-*d*]pyrimidin-2-yl)amino)-1*H*-pyrazol-1-yl)hexanoate (**14x**, 0.15 g, 0.33 mmol) was reacted using a procedure similar to the synthesis of **6a**, affording compound **16e** (0.10 g, 70% yield) as a white solid, mp 140−142 °C. ^{1}H NMR (400 MHz, DMSO-d_6) δ 10.34 (s, 1H), 9.21 (s, 1H), 8.64 (d, J = 17.4 Hz, 2H), 7.93 (s, 1H), 7.50 (s, 1H), 7.26 (d, J = 3.5 Hz, 1H), 7.22−7.09 (m, 4H), 6.41 (d, J = 3.6 Hz, 1H), 5.33 (s, 2H), 4.03 (t, J = 7.0 Hz, 2H), 2.25 (s, 3H), 1.93 (t, J = 7.4 Hz, 2H), 1.80−1.67 (m, 2H), 1.51 (p, J = 7.5 Hz, 2H), 1.21 (tt, J = 9.8, 6.4 Hz, 2H). ^{13}C NMR (101 MHz, DMSO-d_6) δ 169.4, 156.2, 152.2, 151.0, 137.0, 135.6, 129.6, 129.5, 127.6, 126.7, 124.2, 119.1, 111.5, 100.1, 51.7, 47.2, 32.6, 30.3, 26.1, 25.2, 21.1. HRMS (AP-ESI) m/z calcd for $C_{23}H_{27}N_7O_2$ [M + H]$^+$ 434.2299, found 434,2294. Retention time: 7.6 min, eluted with 23% acetonitrile/77% water (containing 0.4% formic acid).

*7-(4-((7-(4-Methylbenzyl)-7H-pyrrolo[2,3-d]pyrimidin-2-yl)-amino)-1H-pyrazol-1-yl)-N-hydroxyheptanamide (**16f**).* Ethyl 7-(4-((7-(4-methylbenzyl)-7*H*-pyrrolo[2,3-*d*]pyrimidin-2-yl)amino)-1*H*-pyrazol-1-yl)heptanoate (**14y**, 0.15 g, 0.32 mmol) was reacted using a procedure similar to the synthesis of **6a**, affording compound **16f** (0.11 g, 70% yield) as a white solid, mp 166−168 °C. ^{1}H NMR (400 MHz, DMSO-d_6) δ 10.35 (s, 1H), 9.20 (s, 1H), 8.62 (s, 2H), 7.94 (s, 1H), 7.50 (s, 1H), 7.25 (d, J = 3.5 Hz, 1H), 7.21−7.09 (m, 4H), 6.41 (d, J = 3.5 Hz, 1H), 5.33 (s, 2H), 4.03 (t, J = 7.0 Hz, 2H), 2.25 (s, 3H), 1.92 (t, J = 7.4 Hz, 2H), 1.72 (t, J = 7.0 Hz, 2H), 1.46 (t, J = 7.2 Hz, 2H), 1.31−1.17 (m, 4H). ^{13}C NMR (101 MHz, DMSO-d_6) δ 169.5, 156.2, 152.2, 151.1, 137.0, 135.6, 129.6, 129.5, 127.6, 126.7, 124.2, 119.1, 111.5, 100.1, 51.7, 47.2, 32.6, 30.4, 28.6, 26.2, 25.5, 21.1. ESI-MS m/z = 448 [M + H]$^+$. HRMS (AP-ESI) m/z calcd for $C_{24}H_{29}N_7O_2$ [M + H]$^+$ 448.2455, found 448.2457. Retention time: 10.4 min, eluted with 23% acetonitrile/77% water (containing 0.4% formic acid).

*6-(4-((7-(4-Methoxybenzyl)-7H-pyrrolo[2,3-d]pyrimidin-2-yl)-amino)-1H-pyrazol-1-yl)-N-hydroxyhexanamide (**16g**).* Ethyl 6-(4-((7-(4-methoxybenzyl)-7*H*-pyrrolo[2,3-*d*]pyrimidin-2-yl)amino)-1*H*-pyrazol-1-yl)hexanoate (**14z**, 0.10 g, 0.21 mmol) was reacted using a procedure similar to the synthesis of **6a**, affording compound **16g** (0.08 g, 95% yield) as a white solid, mp 118−120 °C. ^{1}H NMR (400 MHz, DMSO-d_6) δ 10.36 (s, 1H), 9.23 (s, 1H), 8.70 (s, 1H), 8.62 (s, 1H), 7.97 (s, 1H), 7.52 (s, 1H), 7.29−7.22 (m, 3H), 6.91−6.84 (m, 2H), 6.40 (d, J = 3.5 Hz, 1H), 5.30 (s, 2H), 4.04 (t, J = 6.9 Hz, 2H),

https://dx.doi.org/10.1021/acs.jmedchem.0c02111
J. Med. Chem. XXXX, XXX, XXX−XXX

3.70 (s, 3H), 1.93 (t, J = 7.4 Hz, 2H), 1.74 (t, J = 7.5 Hz, 2H), 1.51 (t, J = 7.5 Hz, 2H), 1.28−1.15 (m, 2H). ^{13}C NMR (101 MHz, DMSO-d_6) δ 169.4, 159.0, 156.2, 152.2, 151.0, 130.5, 129.6, 129.1, 126.6, 124.3, 119.1, 114.4, 111.6, 100.1, 55.5, 51.7, 46.9, 32.6, 30.3, 26.1, 25.2. HRMS (AP-ESI) m/z calcd for $C_{23}H_{27}N_7O_3$ $[M + H]^+$ 450.2248, found 450.2249. Retention time: 4.0 min, eluted with 23% acetonitrile/77% water (containing 0.4% formic acid).

*7-(4-((7-(4-Methoxybenzyl)-7H-pyrrolo[2,3-d]pyrimidin-2-yl)-amino)-1H-pyrazol-1-yl)-N-hydroxyheptanamide (**16h**).* Ethyl 7-(4-((7-(4-methoxybenzyl)-7*H*-pyrrolo[2,3-*d*]pyrimidin-2-yl)amino)-1*H*-pyrazol-1-yl)heptanoate (**14A**, 0.10 g, 0.21 mmol) was reacted using a procedure similar to the synthesis of **6a**, affording compound **16h** (0.08 g, 95% yield) as a white solid, mp 138−140 °C. ^{1}H NMR (600 MHz, DMSO-d_6) δ 10.34 (s, 1H), 9.38 (s, 1H), 8.64 (s, 2H), 7.97 (s, 1H), 7.53 (s, 1H), 7.29 (d, J = 3.5 Hz, 1H), 7.25 (d, J = 8.6 Hz, 2H), 6.89−6.85 (m, 2H), 6.43 (d, J = 3.6 Hz, 1H), 5.30 (s, 2H), 4.04 (t, J = 7.0 Hz, 2H), 3.69 (s, 3H), 1.91 (t, J = 7.4 Hz, 2H), 1.72 (t, J = 7.1 Hz, 2H), 1.44 (q, J = 7.2 Hz, 2H), 1.22 (dq, J = 13.5, 6.9 Hz, 4H). ^{13}C NMR (101 MHz, DMSO-d_6) δ 169.5, 159.0, 156.2, 152.2, 151.0, 130.5, 129.6, 129.1, 126.5, 124.2, 119.1, 114.3, 114.2, 111.5, 100.1, 55.5, 51.7, 46.9, 32.6, 30.4, 28.6, 26.2, 25.5. HRMS (AP-ESI) m/z calcd for $C_{24}H_{29}N_7O_3$ $[M + H]^+$ 464.2405, found 464.2408. Retention time: 5.9 min, eluted with 23% acetonitrile/77% water (containing 0.4% formic acid).

*6-(4-((7-Phenethyl-7H-pyrrolo[2,3-d]pyrimidin-2-yl)amino)-1H-pyrazol-1-yl)-N-hydroxyhexanamide (**16i**).* Ethyl 6-(4-((7-phenethyl-7*H*-pyrrolo[2,3-*d*]pyrimidin-2-yl)amino)-1*H*-pyrazol-1-yl) hexanoate (**14B**, 0.10 g, 0.22 mmol) was reacted using a procedure similar to the synthesis of **6a**, affording compound **16i** (0.08 g, 95% yield) as a white solid, mp 168−170 °C. ^{1}H NMR (400 MHz, DMSO-d_6) δ 10.35 (s, 1H), 9.19 (s, 1H), 8.67 (s, 1H), 8.59 (s, 1H), 7.98 (s, 1H), 7.55 (s, 1H), 7.32−7.19 (m, 5H), 7.19−7.10 (m, 1H), 6.34 (d, J = 3.5 Hz, 1H), 4.38 (dd, J = 8.4, 6.6 Hz, 2H), 4.05 (t, J = 7.0 Hz, 2H), 3.12 (t, J = 7.5 Hz, 2H), 1.93 (t, J = 7.4 Hz, 2H), 1.80−1.71 (m, 2H), 1.55−1.46 (m, 2H), 1.29−1.16 (m, 2H). ^{13}C NMR (101 MHz, DMSO-d_6) δ 169.4, 156.1, 152.2, 150.9, 139.0, 129.7, 129.0, 128.8, 126.8, 126.5, 124.4, 119.0, 99.6, 51.7, 45.4, 35.9, 32.6, 30.2, 26.1, 25.1. HRMS (AP-ESI) m/z calcd for $C_{23}H_{27}N_7O_2$ $[M + H]^+$ 434.2299, found 434.2302. Retention time: 5.9 min, eluted with 25% acetonitrile/75% water (containing 0.4% formic acid).

*7-(4-((7-Phenethyl-7H-pyrrolo[2,3-d]pyrimidin-2-yl)amino)-1H-pyrazol-1-yl)-N-hydroxyheptanamide (**16j**).* Ethyl 7-(4-((7-phenethyl-7*H*-pyrrolo[2,3-*d*]pyrimidin-2-yl)amino)-1*H*-pyrazol-1-yl) heptanoate (**14C**, 0.15 g, 0.32 mmol) was reacted using a procedure similar to the synthesis of **6a**, affording compound **16j** (0.10 g, 70% yield) as a white solid, mp 158−160 °C. ^{1}H NMR (400 MHz, DMSO-d_6) δ 10.36 (s, 1H), 9.41 (s, 1H), 9.18 (s, 1H), 8.59 (s, 1H), 7.99 (s, 1H), 7.55 (s, 1H), 7.32−7.18 (m, 5H), 7.13 (d, J = 3.6 Hz, 1H), 6.34 (d, J = 3.5 Hz, 1H), 4.38 (dd, J = 8.4, 6.5 Hz, 2H), 4.05 (t, J = 7.0 Hz, 2H), 3.12 (dd, J = 8.3, 6.6 Hz, 2H), 1.92 (t, J = 7.4 Hz, 2H), 1.74 (s, 2H), 1.46 (t, J = 7.3 Hz, 2H), 1.24 (p, J = 3.6 Hz, 4H). ^{13}C NMR (101 MHz, DMSO-d_6) δ 169.5, 156.1, 152.2, 150.9, 139.0, 129.7, 129.0, 128.8, 126.8, 126.5, 124.4, 119.1, 111.5, 99.6, 51.8, 45.4, 35.9, 32.6, 30.4, 28.6, 26.2, 25.5. HRMS (AP-ESI) m/z calcd for $C_{24}H_{29}N_7O_2$ $[M + H]^+$ 448.2455, found 448.2454. Retention time: 7.0 min, eluted with 23% acetonitrile/77% water (containing 0.4% formic acid).

*7-(4-((7-Cyclopentyl-7H-pyrrolo[2,3-d]pyrimidin-2-yl)amino)-1H-pyrazol-1-yl)-N-hydroxyheptanamide (**17a**).* Ethyl 7-(4-((7-cyclopentyl-7*H*-pyrrolo[2,3-*d*]pyrimidin-2-yl)amino)-1*H*-pyrazol-1-yl)-heptanoate (**14D**, 0.12 g, 0.28 mmol) was reacted using a procedure similar to the synthesis of **6a**, affording compound **17a** (0.10 g, 86% yield) as a white solid, mp 159−161 °C. ^{1}H NMR (400 MHz, DMSO-d_6) δ 10.30 (s, 1H), 9.13 (s, 1H), 8.63 (s, 1H), 8.57 (s, 1H), 7.92 (s, 1H), 7.54 (s, 1H), 7.24 (d, J = 3.7 Hz, 1H), 6.37 (d, J = 3.6 Hz, 1H), 4.96 (q, J = 7.5 Hz, 1H), 4.03 (t, J = 7.0 Hz, 2H), 2.11 (d, J = 7.9 Hz, 2H), 1.89 (q, J = 6.8, 6.4 Hz, 6H), 1.72 (q, J = 8.4, 7.3 Hz, 4H), 1.50−1.40 (m, 2H), 1.23 (s, 4H). ^{13}C NMR (101 MHz, DMSO-d_6) δ 169.4, 156.0, 150.9, 129.8, 124.4, 124.0, 119.1, 112.0, 99.9, 55.2, 51.7, 32.6, 32.1, 30.3, 28.6, 26.2, 25.4, 24.1. HRMS (AP-ESI) m/z calcd for $C_{21}H_{30}N_7O_2$ $[M + H]^+$ 412.2455, found 412.2444. Retention time: 4.8 min, eluted with 23% acetonitrile/77% water (containing 0.4% formic acid).

*7-(4-((7-(Cyclopropylmethyl)-7H-pyrrolo[2,3-d]pyrimidin-2-yl)-amino)-1H-pyrazol-1-yl)-N-hydroxyheptanamide (**17b**).* Ethyl 7-(4-((7-(cyclopropylmethyl)-7*H*-pyrrolo[2,3-*d*]pyrimidin-2-yl)amino)-1*H*-pyrazol-1-yl)heptanoate (**14E**, 0.08 g, 0.19 mmol) was reacted using a procedure similar to the synthesis of **6a**, affording compound **17b** (0.06 g, 77% yield) as a white solid, mp 135−137 °C. ^{1}H NMR (400 MHz, DMSO-d_6) δ 10.30 (s, 1H), 9.14 (s, 1H), 8.64 (d, J = 1.7 Hz, 1H), 8.59 (s, 1H), 7.95 (s, 1H), 7.53 (s, 1H), 7.23 (d, J = 3.6 Hz, 1H), 6.36 (d, J = 3.6 Hz, 1H), 4.08−3.95 (m, 4H), 1.91 (t, J = 7.4 Hz, 2H), 1.79−1.67 (m, 2H), 1.44 (q, J = 7.2 Hz, 2H), 1.23 (q, J = 8.1, 4.7 Hz, 5H), 0.48 (dtd, J = 7.8, 6.1, 5.5, 2.7 Hz, 2H), 0.42 (tt, J = 5.1, 2.6 Hz, 2H). ^{13}C NMR (126 MHz, DMSO-d_6) δ 169.5, 156.2, 152.2, 150.9, 129.7, 126.5, 124.4, 119.1, 99.6, 51.7, 48.2, 32.6, 30.3, 28.6, 26.2, 25.4. 11.9. HRMS (AP-ESI) m/z calcd for $C_{20}H_{28}N_7O_2$ $[M + H]^+$ 398.2299, found 398.2308. Retention time: 2.7 min, eluted with 23% acetonitrile/77% water (containing 0.4% formic acid).

*7-(4-((7-(Cyclohexylmethyl)-7H-pyrrolo[2,3-d]pyrimidin-2-yl)-amino)-1H-pyrazol-1-yl)-N-hydroxyheptanamide (**17c**).* Ethyl 7-(4-((7-(cyclohexylmethyl)-7*H*-pyrrolo[2,3-*d*]pyrimidin-2-yl)amino)-1*H*-pyrazol-1-yl)heptanoate (**14F**, 0.10 g, 0.22 mmol) was reacted using a procedure similar to the synthesis of **6a**, affording compound **17c** (0.08 g, 82% yield) as a white solid, mp 142−144 °C. ^{1}H NMR (400 MHz, DMSO-d_6) δ 10.32 (s, 1H), 9.17 (s, 1H), 8.63 (s, 1H), 8.58 (s, 1H), 7.99 (s, 1H), 7.50 (s, 1H), 7.14 (d, J = 3.6 Hz, 1H), 6.35 (d, J = 3.5 Hz, 1H), 4.03 (t, J = 7.0 Hz, 2H), 3.97 (d, J = 7.1 Hz, 2H), 1.90 (t, J = 7.4 Hz, 3H), 1.73 (s, 2H), 1.64 (s, 2H), 1.61−1.51 (m, 3H), 1.49−1.41 (m, 2H), 1.23 (s, 4H), 1.17−1.07 (m, 3H), 0.99 (d, J = 12.1 Hz, 2H). ^{13}C NMR (126 MHz, DMSO-d_6) δ 169.4, 156.1, 152.5, 150.9, 129.5, 127.1, 124.5, 118.9, 111.4, 99.4, 51.8, 50.1, 38.4, 32.6, 30.8, 30.4, 28.6, 26.4, 26.3, 25.6, 25.4. HRMS (AP-ESI) m/z calcd for $C_{23}H_{34}N_7O_2$ $[M + H]^+$ 440.2768, found 440.2766. Retention time: 16.7 min, eluted with 23% acetonitrile/77% water (containing 0.4% formic acid).

Molecular Docking Study. The crystal structures of JAK2 (PDB 3FUP) and HDAC6 (PDB 5EEI) were obtained from the Protein Data Bank. Before the docking process, the structure of protein was treated by adding hydrogen atoms, deleting water molecules, assigning AMBER7 FF99 charges, and a 100-step minimization process using Sybyl X_2.1. The molecular structure was generated with the Sybyl/Sketch module and optimized using Powell's method with the Tripos force field with convergence criterion set at 0.005 kcal/(Å mol) and assigned charges with the Gasteiger−Hückel method. Other docking parameters were kept to the default values. Molecular docking was carried out via the Sybyl/Surflex-Dock module.

Janus Kinase Inhibition Assay. (1) Janus kinase 1/2/3 inhibition assay. Target compounds were dissolved in DMSO and centrifuged for 5 min to obtain 10^{-2} M solution. The 10^{-2} M target compound solutions were kept at 4 °C. The final concentration of DMSO in the assay was no more than 1%. In 384-well plates, a 5 μL enzyme system (50 mM HEPES pH 7.5, 1 mM EGTA, 10 mM $MgCl_2$, 0.01% brij-35, 4 μM substrate, 0.4−5 ng/μL enzymes) was added with 2.5 μL of target compound solution, 2.5 μL of 200 μM ATP. The mixture was incubated at room temperature and away from light for 60 min. Subsequently, 5 μL of reagent A diluted with development buffer was added to each well and incubated at room temperature and away from light for 60 min. Then, 5 μL of stop solution was added to each well to terminate the reaction and incubated at room temperature and away from light for 10 min. Fluorescence intensity was measured using a microplate reader at excitation and emission wavelengths of 400 and 445/520 nm, respectively. Origin data analysis software were used to calculate the IC_{50} data by the nonlinear curve fitting method (allowed to float and fitted as a parameter). (2) TYK2 kinase inhibition assay. Target compounds were dissolved in DMSO and centrifuged for 5 min to obtain 10^{-2} M solution. The 10^{-2} M target compound solutions were kept at 4 °C. The final concentration of DMSO in the assay was no more than 1%. In 384-well plates, 3 μL of enzyme system (5 mM

https://dx.doi.org/10.1021/acs.jmedchem.0c02111
J. Med. Chem. XXXX, XXX, XXX−XXX

$MgCl_2$, 1 mM $MnCl_2$, 1 mM DTT, 12.5 nM SEB, 0.8 ng/μL enzyme) was added with 4 μL of target compound solution, 3 μL of substrate mixture (33.3 μM ATP and 3.3 μM substrate) and incubated at room temperature for 40 min. Subsequently, 10 μL of premix of SA-XL665 and TK Ab was added to stop the reaction and incubated the plate at room temperature for 1 h and then read in a microplate reader using HTRF settings. GraphPad software were used to calculate the IC_{50} data by the nonlinear curve fitting method (allowed to float and fitted as a parameter).

Protein Kinase Selectivity Profile. The kinase inhibition assays were performed by Eurofins Cerep Corporation in France. In brief, evaluation of the effects of compounds on the activity of the kinases was quantified by measuring the phosphorylation of their substrates using human recombinant enzymes and the LANCE detection method. For example, evaluation of the effects of compounds on the activity of the human ALK quantified by measuring the phosphorylation of the substrate Ulight-CKKSRGDYMTMQIG (IRS-1) using a human recombinant enzyme and the LANCE detection method. The test compound, reference compound or water (control) were mixed with the enzyme (about 0.25 ng) in a buffer containing 40 mM Hepes/Tris (pH 7.4), 0.8 mM EGTA/Tris, 8 mM $MgCl_2$, 1.6 mM DTT, and 0.008% Tween 20. Thereafter, the reaction is initiated by adding 250 nM of the substrate Ulight-CKKSRGDYMTMQIG (IRS-1) and 30 μM ATP, and the mixture is incubated for 60 min at room temperature. For control basal measurements, the enzyme is omitted from the reaction mixture. Following incubation, the reaction is stopped by adding 13 mM EDTA. After 5 min, the antiphopho-PT66 antibody labeled with europium chelate is added. After 60 more min, the fluorescence transfer is measured at excitation and emission wavelengths of 337 and 620/665 nm, using a microplate reader (Envision, PerkinElmer). The enzyme activity is determined by dividing the signal measured at 665 nm by that measured at 620 nm (ratio). The results are expressed as a percent inhibition of the control enzyme activity. Other kinase inhibition assays were performed as above method.

In Vitro HDAC1/6 Inhibition Fluorescence Assay. In 384-well plates, 5 μL of enzyme system (15 mM Tris-HCl pH 8.1, 250 μM EDTA, 250 mM NaCl, 10% glycerol, 0.7−12.5 ng/μL enzymes) was added with 2.5 μL of target compound solution and 2.5 μL of substrate. The mixture was incubated at room temperature protected from light for 60 min. Subsequently, 10 μL of trypsin diluted with trypsin buffer was added to each well and incubated at room temperature and away from light for 10 min. Fluorescence intensity was measured using a microplate reader at excitation and emission wavelengths of 390 and 460 nm, respectively. The inhibition ratios were calculated from the fluorescence intensity readout of tested wells relative to those of control wells, and the IC_{50} values were calculated using Prism nonlinear curve fitting method (allowed to float and fitted as a parameter).

In Vitro HDAC3 Enzymic Assay. A 10 μL reactive system (50 mM Tris-HCl, pH 8.0, 137 mM NaCl, 2.7 mM KCl, 1 mM $MgCl_2$, 0.01% Tween20) containing HDAC3 enzyme, H3(1−21)K9Ac substrate, and the tested compounds was added in 384-well plates and incubated at room temperature for 1 h. Subsequently, 10 μL of premix of SA-XL665 and anti-H3K9me0-Eu(K) was added to stop the reaction and incubated the plate at room temperature for 1 h and then read in a microplate reader using HTRF settings. GraphPad software were used to calculate the IC_{50} data by the nonlinear curve fitting method (allowed to float and fitted as a parameter).

In Vitro HDAC4, HDAC7, HDAC8, and HDAC10 Enzymic Assay. The assays were carried out by Sundia MediTech Company, Ltd. Briefly, different concentrations of compounds were incubated with recombinant HDAC4, HDAC7, HDAC8 (Active Motif, USA), and HDAC10 (BPS Biosciences, USA) at room temperature for 15 min, which was followed by adding mixture of Ac-peptide-AMC substrates to initiate the coupled reaction in Tris-based assay buffer. For HDAC4 and HDAC7, fluorescent AMC released from substrate was measured in Synergy2 (BioTek, US) using filter sets as excitation = 355 nm and emission = 460 nm kinetically. For HDAC8 and HDAC10, reaction mixtures were incubated at room temperature for 240 min. Then stop solution containing trypsin was added. The coupled reaction was incubated for another 90 min at 37 °C. Fluorescent AMC released from substrate was measured in Synergy2 using filter sets as excitation = 355 nm and emission = 460 nm. IC_{50} values were calculated by GraphPad Prism software (California, US).

Western Blot Analysis. Cells in the logarithmic growth stage were inoculated into 6-well culture plates at an appropriate density overnight before exposed to compounds of different concentrations. After treatment, cells were collected and lysed using 1× SDS sample buffer (50 mM Tris pH 6.8, 100 mM DTT, 2% SDS, 0.1% bromophenol blue, 10% glycerol). The cell lysate was collected, heated in a boiling water bath for 10 min, and centrifuged at 10 000 rpm for 10 min. The supernatant was taken for SDS-page electrophoresis. After the electrophoresis, the proteins were transferred to the cellulose nitrate membrane. The membrane was incubated in sealing solution containing 5% skim milk powder (5% skim milk, 20 mM tris-HCl PH 7.2−7.4, 150 mM NaCl, 0.1% Tween-20) for 60 min at room temperature. and then placed in a primary antibody diluted in 5% skim milk at 4 °C overnight. After washing with 100 mM tris-HCl (PH. 7.2−7.4, 0.9% NaCl, 0.2% Tween-20) at room temperature for 3 times, 10 min each, horseradish peroxidase-labeled secondary antibody was added and incubated at room temperature for 1 h. After three-time washing, and the blots were visualized with an enhanced chemiluminescence assay.

In Vitro Antiproliferative Assay. SRB assay was used to determine the growth inhibition of cancer cells. The specific steps were as follows: 100 μL cells in the logarithmic growth stage were seeded to the 96-well culture plate according to the appropriate density and incubated overnight. Different concentrations of compounds were added and coincubated for 72 h. After the coincubation, pour the culture solution and add 10% (w/v) trichloroacetic acid (100 μL/well) at 4 °C for 1 h. Then the adherent cells were washed with distilled water five times. After drying by air, to each well was added 100 μL of SRB solution (Sigma, st. Louis, MO, U.S.A) (4 mg/mL, soluble in 1% acetic acid). After incubation for 15 min, it was washed with 1% acetic acid for five times. After drying by air, 10 mM Tris solution (100 μL) was added to each well, and the optical density (OD value) at the wavelength of 560 nm was determined by SPECTRA max PLUS.

Apoptosis Assay. For flow cytometry assay, annexin V-FITC/propidium iodide (PI) staining assay (A211-02, Vazyme) was employed to detect cells in early apoptotic and late apoptotic stages. Cells were seeded in 6-well plates and incubated overnight, then treated with DMSO or compounds for 48 h, and harvested and washed in cold PBS. Cells were resuspended in 100 μL of annexin V-FITC/PI staining solution and incubated for 10−15 min at room temperature. After incubation, the cells were collected and analyzed by FACSCalibur (BD, USA), and data were analyzed using FlowJo 7.6 Software.

In Vivo Antitumor Activity Assay. The female BALB/c nude mice (IACUC no. 2019-04-GMY-12) were purchased from Beijing Vital River Laboratory Animal Technology Co. Ltd. MDA-MB-231 cells were suspended in serum-free medium and injected with 0.2 mL containing 2×10^6 cells into the right flank of BALB/c-nude mice. When the tumor reached a mean volume of 100−150 mm^3, the tumor-bearing nude mice were randomly divided into control and treatment groups (6 mice/group) and received the vehicle, SAHA (100 mg/kg/d, PO), ruxolintinib (100 mg/kg/d, PO), and **15d** (30 and 100 mg/kg/d, IP) at indicated doses. The size of tumors was measured individually twice per week. Tumor volume (TV) was calculated as $V = (\text{length} \times \text{width}^2)/2$. All experiments were performed according to the institutional ethical guidelines on animal care and approved by the Institute Animal Care and Use Committee at Shanghai Institute of Materia Medica.

■ ASSOCIATED CONTENT

Supporting Information

The Supporting Information is available free of charge at https://pubs.acs.org/doi/10.1021/acs.jmedchem.0c02111.

https://dx.doi.org/10.1021/acs.jmedchem.0c02111
J. Med. Chem. XXXX, XXX, XXX−XXX

Supporting tables; ^{1}H NMR, and ^{13}C NMR of all target compounds; HPLC spectra and HRMS of the representative compounds (PDF)
Molecular formula stings (CSV) (CSV)
Predicted binding mode of **6a** in the ATP pocket of JAK2; surface representation of **6a** in the ATP pocket of JAK2 (3FUP) (PDB)
Predicted binding mode of **15d** in the ATP pocket of JAK2 (3FUP) (PDB)
Predicted binding mode of **16b** in the ATP pocket of JAK2 (3FUP) (PDB)
Predicted binding mode of **6a** in the active site of HDAC6; surface representation of **6a** in the active site of HDAC6 (5EEI) (PDB)
Predicted binding mode of **15d** in the active site of HDAC6 (5EEI) (PDB)
Predicted binding mode of **16b** in the active site of HDAC6 (5EEI) (PDB)

AUTHOR INFORMATION

Corresponding Authors

Hong Liu − *State Key Laboratory of Drug Research, Shanghai Institute of Materia Medica, Chinese Academy of Sciences, Shanghai 201203, China;* orcid.org/0000-0003-3685-6268; Phone: +86 21 50807042; Email: hliu@mail.shcnc.ac.cn

Min Huang − *State Key Laboratory of Drug Research, Shanghai Institute of Materia Medica, Chinese Academy of Sciences, Shanghai 201203, China*; Email: mhuang@simm.ac.cn

Authors

Xuewu Liang − *State Key Laboratory of Drug Research, Shanghai Institute of Materia Medica, Chinese Academy of Sciences, Shanghai 201203, China*

Shuai Tang − *State Key Laboratory of Drug Research, Shanghai Institute of Materia Medica, Chinese Academy of Sciences, Shanghai 201203, China*

Xuyi Liu − *State Key Laboratory of Drug Research, Shanghai Institute of Materia Medica, Chinese Academy of Sciences, Shanghai 201203, China*

Yingluo Liu − *State Key Laboratory of Drug Research, Shanghai Institute of Materia Medica, Chinese Academy of Sciences, Shanghai 201203, China*

Qifu Xu − *Department of Medicinal Chemistry, School of Pharmacy, Shandong University, Ji'nan, Shandong 250012, P. R. China*

Xiaomin Wang − *State Key Laboratory of Drug Research, Shanghai Institute of Materia Medica, Chinese Academy of Sciences, Shanghai 201203, China*

Abdusaid Saidahmatov − *State Key Laboratory of Drug Research, Shanghai Institute of Materia Medica, Chinese Academy of Sciences, Shanghai 201203, China*

Chunpu Li − *State Key Laboratory of Drug Research, Shanghai Institute of Materia Medica, Chinese Academy of Sciences, Shanghai 201203, China*

Jiang Wang − *State Key Laboratory of Drug Research, Shanghai Institute of Materia Medica, Chinese Academy of Sciences, Shanghai 201203, China*

Yu Zhou − *State Key Laboratory of Drug Research, Shanghai Institute of Materia Medica, Chinese Academy of Sciences, Shanghai 201203, China;* orcid.org/0000-0002-7684-2939

Yingjie Zhang − *Department of Medicinal Chemistry, School of Pharmacy, Shandong University, Ji'nan, Shandong 250012, P. R. China;* orcid.org/0000-0001-6118-6695

Meiyu Geng − *State Key Laboratory of Drug Research, Shanghai Institute of Materia Medica, Chinese Academy of Sciences, Shanghai 201203, China*

Complete contact information is available at: https://pubs.acs.org/10.1021/acs.jmedchem.0c02111

Author Contributions

X.W. Liang and S. Tang, contributed equally to this work. All authors have given approval to the final version of the manuscript.

Notes

The authors declare no competing financial interest.

ACKNOWLEDGMENTS

This study was supported by National Natural Science Foundation of China (21907102, 21632008, 91229204, 81473245, and 81772695).

ABBREVIATIONS USED

AML, acute myelocytic leukemia; CTCL, cutaneous T cell lymphoma; EL, erythroleukemia cell lines; HDACs, histone deacetylases; JAK, Janus kinase; LIFR, leukemia inhibitory factor receptor; MM, multiple myeloma; INCB, ruxolitinib; SAR, structure−activity relationship; SRC, surface recognition cap; STAT, signal transducers and activators of transcription; ZBG, zinc-binding group

REFERENCES

(1) Tan, Z.; Zhang, S. Past, present, and future of targeting Ras for cancer therapies. *Mini-Rev. Med. Chem.* **2016**, *16*, 345−357.
(2) Tan, Z.; Chaudhai, R.; Zhang, S. Polypharmacology in drug development: A minireview of current technologies. *ChemMedChem* **2016**, *11*, 1211−1218.
(3) Zimmermann, G. R.; Lehar, J.; Keith, C. T. Multi-target therapeutics: when the whole is greater than the sum of the parts. *Drug Discovery Today* **2007**, *12*, 34−42.
(4) Morphy, R.; Rankovic, Z. Designed multiple ligands. An emerging drug discovery paradigm. *J. Med. Chem.* **2005**, *48*, 6523−6543.
(5) Csermely, P.; Agoston, V.; Pongor, S. The efficiency of multi-target drugs: the network approach might help drug design. *Trends Pharmacol. Sci.* **2005**, *26*, 178−182.
(6) Hartman, J. L. t.; Garvik, B.; Hartwell, L. Principles for the buffering of genetic variation. *Science* **2001**, *291*, 1001−1004.
(7) Hesham, H. M.; Lasheen, D. S.; Abouzid, K. A. M. Chimeric HDAC inhibitors: Comprehensive review on the HDAC-based strategies developed to combat cancer. *Med. Res. Rev.* **2018**, *38*, 2058−2109.
(8) Xu, W. S.; Parmigiani, R. B.; Marks, P. A. Histone deacetylase inhibitors: molecular mechanisms of action. *Oncogene* **2007**, *26*, 5541−5552.
(9) He, S.; Dong, G.; Li, Y.; Wu, S.; Wang, W.; Sheng, C. Potent dual BET/HDAC inhibitors for efficient treatment of pancreatic cancer. *Angew. Chem., Int. Ed.* **2020**, *59*, 3028−3032.
(10) Liang, X.; Liu, H.; Zhang, Y. Novel-targeted therapy for hematological malignancies with JAK and HDAC dual inhibitors. *Future Med. Chem.* **2019**, *11*, 1849−1852.
(11) Slingerland, M.; Guchelaar, H. J.; Gelderblom, H. Histone deacetylase inhibitors: an overview of the clinical studies in solid tumors. *Anti-Cancer Drugs* **2014**, *25*, 140−149.

(12) Stadler, W. M.; Margolin, K.; Ferber, S.; McCulloch, W.; Thompson, J. A. A phase II study of depsipeptide in refractory metastatic renal cell cancer. *Clin. Genitourin. Cancer* **2006**, *5*, 57−60.
(13) Molife, L. R.; Attard, G.; Fong, P. C.; Karavasilis, V.; Reid, A. H.; Patterson, S.; Riggs, C. E., Jr.; Higano, C.; Stadler, W. M.; McCulloch, W.; Dearnaley, D.; Parker, C.; de Bono, J. S. Phase II, two-stage, single-arm trial of the histone deacetylase inhibitor (HDACi) romidepsin in metastatic castration-resistant prostate cancer (CRPC). *Ann. Oncol* **2010**, *21*, 109−113.
(14) Haigentz, M., Jr.; Kim, M.; Sarta, C.; Lin, J.; Keresztes, R. S.; Culliney, B.; Gaba, A. G.; Smith, R. V.; Shapiro, G. I.; Chirieac, L. R.; Mariadason, J. M.; Belbin, T. J.; Greally, J. M.; Wright, J. J.; Haddad, R. I. Phase II trial of the histone deacetylase inhibitor romidepsin in patients with recurrent/metastatic head and neck cancer. *Oral Oncol.* **2012**, *48*, 1281−1288.
(15) Liu, T.; Wan, Y.; Xiao, Y.; Xia, C.; Duan, G. Dual-target inhibitors based on HDACs: novel antitumor agents for cancer therapy. *J. Med. Chem.* **2020**, *63*, 8977−9002.
(16) Mahboobi, S.; Sellmer, A.; Winkler, M.; Eichhorn, E.; Pongratz, H.; Ciossek, T.; Baer, T.; Maier, T.; Beckers, T. Novel chimeric histone deacetylase inhibitors: a series of lapatinib hybrides as potent inhibitors of epidermal growth factor receptor (EGFR), human epidermal growth factor receptor 2 (HER2), and histone deacetylase activity. *J. Med. Chem.* **2010**, *53*, 8546−8555.
(17) Peng, F. W.; Xuan, J.; Wu, T. T.; Xue, J. Y.; Ren, Z. W.; Liu, D. K.; Wang, X. Q.; Chen, X. H.; Zhang, J. W.; Xu, Y. G.; Shi, L. Design, synthesis and biological evaluation of N-phenylquinazolin-4-amine hybrids as dual inhibitors of VEGFR-2 and HDAC. *Eur. J. Med. Chem.* **2016**, *109*, 1−12.
(18) Zang, J.; Liang, X.; Huang, Y.; Jia, Y.; Li, X.; Xu, W.; Chou, C. J.; Zhang, Y. Discovery of novel Pazopanib-based HDAC and VEGFR dual inhibitors targeting cancer epigenetics and angiogenesis simultaneously. *J. Med. Chem.* **2018**, *61*, 5304−5322.
(19) Ko, K. S.; Steffey, M. E.; Brandvold, K. R.; Soellner, M. B. Development of a chimeric c-Src kinase and HDAC inhibitor. *ACS Med. Chem. Lett.* **2013**, *4*, 779−783.
(20) Makarevic, J.; Rutz, J.; Juengel, E.; Maxeiner, S.; Mani, J.; Vallo, S.; Tsaur, I.; Roos, F.; Chun, F. K.; Blaheta, R. A. HDAC inhibition counteracts metastatic re-activation of prostate cancer cells induced by chronic mTOR suppression. *Cells* **2018**, *7*, 129−146.
(21) Terranova-Barberio, M.; Thomas, S.; Ali, N.; Pawlowska, N.; Park, J.; Krings, G.; Rosenblum, M. D.; Budillon, A.; Munster, P. N. HDAC inhibition potentiates immunotherapy in triple negative breast cancer. *Oncotarget* **2017**, *8*, 114156−114172.
(22) Zeng, H.; Qu, J.; Jin, N.; Xu, J.; Lin, C.; Chen, Y.; Yang, X.; He, X.; Tang, S.; Lan, X.; Yang, X.; Chen, Z.; Huang, M.; Ding, J.; Geng, M. Feedback activation of leukemia inhibitory factor receptor limits response to histone deacetylase inhibitors in breast cancer. *Cancer Cell* **2016**, *30*, 459−473.
(23) Clark, J. D.; Flanagan, M. E.; Telliez, J. B. Discovery and development of janus kinase (JAK) inhibitors for inflammatory diseases. *J. Med. Chem.* **2014**, *57*, 5023−5038.
(24) Pellegrini, S.; Dusanter-Fourt, I. The structure, regulation and function of the janus kinases (JAKs) and the signal transducers and activators of transcription (STATs). *Eur. J. Biochem.* **1997**, *248*, 615−633.
(25) Nosaka, T.; Kitamura, T. Janus kinases (JAKs) and signal transducers and activators of transcription (STATs) in hematopoietic cells. *Int. J. Hematol.* **2000**, *71*, 309−319.
(26) Yamaoka, K.; Saharinen, P.; Pesu, M.; Holt, V. E.; Silvennoinen, O.; O'Shea, J. J. The janus kinases (Jaks). *Genome Biol.* **2004**, *5*, 253.
(27) Yang, E. G.; Mustafa, N.; Tan, E. C.; Poulsen, A.; Ramanujulu, P. M.; Chng, W. J.; Yen, J. J.; Dymock, B. W. Design and synthesis of Janus kinase 2 (JAK2) and histone deacetlyase (HDAC) bispecific inhibitors based on Pacritinib and evidence of dual pathway inhibition in hematological cell lines. *J. Med. Chem.* **2016**, *59*, 8233−8262.
(28) Yao, L.; Mustafa, N.; Tan, E. C.; Poulsen, A.; Singh, P.; Duong-Thi, M. D.; Lee, J. X. T.; Ramanujulu, P. M.; Chng, W. J.; Yen, J. J. Y.; Ohlson, S.; Dymock, B. W. Design and synthesis of ligand efficient dual inhibitors of Janus kinase (JAK) and histone deacetylase (HDAC) based on ruxolitinib and vorinostat. *J. Med. Chem.* **2017**, *60*, 8336−8357.
(29) Chu-Farseeva, Y. Y.; Mustafa, N.; Poulsen, A.; Tan, E. C.; Yen, J. J. Y.; Chng, W. J.; Dymock, B. W. Design and synthesis of potent dual inhibitors of JAK2 and HDAC based on fusing the pharmacophores of XL019 and vorinostat. *Eur. J. Med. Chem.* **2018**, *158*, 593−619.
(30) Huang, Y.; Dong, G.; Li, H.; Liu, N.; Zhang, W.; Sheng, C. Discovery of janus kinase 2 (JAK2) and histone deacetylase (HDAC) dual inhibitors as a novel strategy for the combinational treatment of leukemia and invasive fungal infections. *J. Med. Chem.* **2018**, *61*, 6056−6074.
(31) Liang, X.; Zang, J.; Li, X.; Tang, S.; Huang, M.; Geng, M.; Chou, C. J.; Li, C.; Cao, Y.; Xu, W.; Liu, H.; Zhang, Y. Discovery of novel janus kinase (JAK) and histone deacetylase (HDAC) dual inhibitors for the treatment of hematological malignancies. *J. Med. Chem.* **2019**, *62*, 3898−3923.
(32) Kulagowski, J. J.; Blair, W.; Bull, R. J.; Chang, C.; Deshmukh, G.; Dyke, H. J.; Eigenbrot, C.; Ghilardi, N.; Gibbons, P.; Harrison, T. K.; Hewitt, P. R.; Liimatta, M.; Hurley, C. A.; Johnson, A.; Johnson, T.; Kenny, J. R.; Bir Kohli, P.; Maxey, R. J.; Mendonca, R.; Mortara, K.; Murray, J.; Narukulla, R.; Shia, S.; Steffek, M.; Ubhayakar, S.; Ultsch, M.; van Abbema, A.; Ward, S. I.; Waszkowycz, B.; Zak, M. Identification of imidazo-pyrrolopyridines as novel and potent JAK1 inhibitors. *J. Med. Chem.* **2012**, *55*, 5901−5921.
(33) Su, Q.; Ioannidis, S.; Chuaqui, C.; Almeida, L.; Alimzhanov, M.; Bebernitz, G.; Bell, K.; Block, M.; Howard, T.; Huang, S.; Huszar, D.; Read, J. A.; Rivard Costa, C.; Shi, J.; Su, M.; Ye, M.; Zinda, M. Discovery of 1-methyl-1H-imidazole derivatives as potent Jak2 inhibitors. *J. Med. Chem.* **2014**, *57*, 144−158.

https://dx.doi.org/10.1021/acs.jmedchem.0c02111
J. Med. Chem. XXXX, XXX, XXX−XXX